

MODIS observations of cyanobacterial risks in a eutrophic lake: Implications for long-term safety evaluation in drinking-water source

This is the peer reviewed version of the following article:

Original:

Duan, H., Tao, M., Loisel, S.A., Zhao, W., Cao, Z., Ma, R., et al. (2017). MODIS observations of cyanobacterial risks in a eutrophic lake: Implications for long-term safety evaluation in drinking-water source. WATER RESEARCH, 122, 455-470 [10.1016/j.watres.2017.06.022].

Availability:

This version is available <http://hdl.handle.net/11365/1033421> since 2018-02-23T13:19:06Z

Published:

DOI:10.1016/j.watres.2017.06.022

Terms of use:

Open Access

The terms and conditions for the reuse of this version of the manuscript are specified in the publishing policy. Works made available under a Creative Commons license can be used according to the terms and conditions of said license.

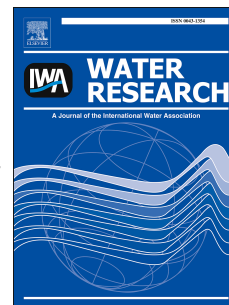
For all terms of use and more information see the publisher's website.

(Article begins on next page)

Accepted Manuscript

MODIS observations of cyanobacterial risks in a eutrophic lake: Implications for long-term safety evaluation in drinking-water source

Hongtao Duan, Min Tao, Steven Arthur Loiselle, Wei Zhao, Zhigang Cao, Ronghua Ma, Xiaoxian Tang



PII: S0043-1354(17)30498-0

DOI: [10.1016/j.watres.2017.06.022](https://doi.org/10.1016/j.watres.2017.06.022)

Reference: WR 12977

To appear in: *Water Research*

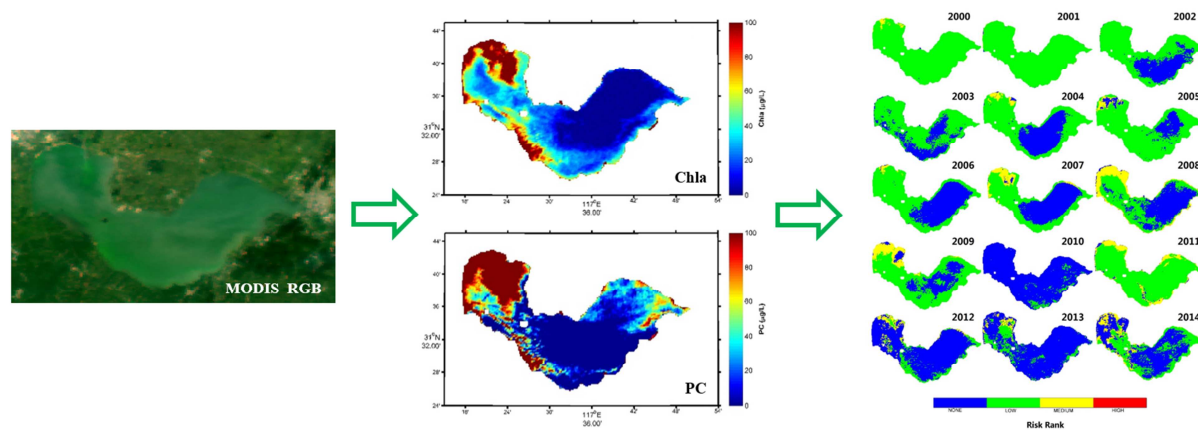
Received Date: 31 March 2017

Revised Date: 6 June 2017

Accepted Date: 7 June 2017

Please cite this article as: Duan, H., Tao, M., Loiselle, S.A., Zhao, W., Cao, Z., Ma, R., Tang, X., MODIS observations of cyanobacterial risks in a eutrophic lake: Implications for long-term safety evaluation in drinking-water source, *Water Research* (2017), doi: 10.1016/j.watres.2017.06.022.

This is a PDF file of an unedited manuscript that has been accepted for publication. As a service to our customers we are providing this early version of the manuscript. The manuscript will undergo copyediting, typesetting, and review of the resulting proof before it is published in its final form. Please note that during the production process errors may be discovered which could affect the content, and all legal disclaimers that apply to the journal pertain.



**MODIS observations of cyanobacterial risks in a eutrophic lake:
implications for long-term safety evaluation in drinking-water
source**

Hongtao Duan ^{a,*}, Min Tao ^a, Steven Arthur Loiselle ^b, Wei Zhao ^c, Zhigang Cao ^a, Ronghua
Ma ^a, and Xiaoxian Tang ^d

6

^a *Key Laboratory of Watershed Geographic Sciences, Nanjing Institute of Geography and
Limnology, Chinese Academy of Sciences, Nanjing 210008, China*

^b *Dipartimento Farmaco Chimico Tecnologico, CSGI, University of Siena, 53100 Siena,
Italy*

^c *Nanjing Institute of Environmental Sciences, Ministry of Environmental Protection,
Nanjing 210042, China*

^d *Monitoring Station of Chaohu Lake Management Authority, Chaohu 238000, China*

14

*Corresponding author: Hongtao Duan

Email: hduan@niglas.ac.cn; Phone: 86-25-86882161

Abstract:

The occurrence and related risks from cyanobacterial blooms have increased world-wide over the past 40 years. Information on the abundance and distribution of cyanobacteria is fundamental to support risk assessment and management activities. In the present study, an approach based on Empirical Orthogonal Function (EOF) analysis was used to estimate the concentrations of chlorophyll a (Chla) and the cyanobacterial biomarker pigment phycocyanin (PC) using data from the MODerate resolution Imaging Spectroradiometer (MODIS) in Lake Chaohu (China's fifth largest freshwater lake). The approach was developed and tested using fourteen years (2000–2014) of MODIS images, which showed significant spatial and temporal variability of the PC:Chla ratio, an indicator of cyanobacterial dominance. The results had unbiased RMS uncertainties of <60% for Chla ranging between 10 and 300 µg/L, and unbiased RMS uncertainties of <65% for PC between 10 and 500 µg/L. Further analysis showed the importance of nutrient and climate conditions for this dominance. Low TN:TP ratios (<29:1) and elevated temperatures were found to influence the seasonal shift of phytoplankton community. The resultant MODIS Chla and PC products were then used for cyanobacterial risk mapping with a decision tree classification model. The resulting Water Quality Decision Matrix (WQDM) was designed to assist authorities in the identification of possible intake areas, as well as specific months when higher frequency monitoring and more intense water treatment would be required if the location of the present intake area remained the same. Remote sensing cyanobacterial risk mapping provides a new tool for reservoir and lake management programs.

Keywords: Remote sensing; PC; Algal bloom; Lake Chaohu; Cyanobacterial dominance

I. Introduction

Freshwater is one of the planet's most valuable resources and an essential life-sustaining element and necessary for the survival of nearly all ecosystems. However, insufficient availability and ongoing degradation of this resource is threatening 1.1 billion people around the globe (UN 2006). One growing threat is the increasing frequency of cyanobacterial blooms in freshwater lakes and reservoirs (Chorus and Bartram 1999, Paerl et al. 2011), 87% of the surface freshwater suitable for drinking (Schneider 1996). Cyanobacteria can produce a variety of toxins with negative effects on human health and aquatic life (WHO 2011). The threat posed by cyanobacterial blooms has increased over the past 40 years (Chorus and Bartram 1999, Duan et al. 2009, O'Neil et al. 2012).

With increased population pressure and depleted groundwater reserves, surface water both from rivers and lakes/reservoirs is becoming more used as a raw water source (Falconer and Humpage 2005). The monitoring of water bodies and freshwater supply systems for cyanobacteria and cyanotoxins is not yet common practice in most countries in the world, as sampling and analysis are time-consuming and labor intensive (Chorus and Bartram 1999, Hunter et al. 2010). There is a clear need for timely detection and quantification of cyanobacterial blooms to control public health risks due to compromised drinking-water sources.

Remote estimation of the concentrations of phytoplankton pigments provides helpful

information to assess the risk of cyanobacterial blooms. The estimation of Chlorophyll *a* (Chl_a) has been used to provide basic information on plankton biomass and its distribution has been used for decades (Morel and Prieur 1977), but cannot be used to specifically determine the abundance of cyanobacteria when other phytoplankton groups co-occur (Duan et al. 2012a, Hunter et al. 2009). The estimation of phycocyanin (PC) is a good indicator of cyanobacteria biomass, but is often more challenging in optically complex waters (Bresciani et al. 2014, Qi et al. 2014b, Simis et al. 2005). The relative contribution of cyanobacteria to total phytoplankton biomass, the ratio of the PC to Chl_a concentrations (PC:Chl_a), can be used to indicate cyanobacterial dominance (Duan et al. 2012a, Shi et al. 2015a, Simis et al. 2007). Specifically, remotely sensed Chl_a and PC:Chl_a products are used in risk assessment models based upon the World Health Organization guidance levels for recreational waterbodies (Hunter et al. 2009, Shi et al. 2015a). This suggests that remote sensing might be able to make a significant contribution to cyanobacterial hazard identification and risk assessment.

There are a number of sensors designed for ocean color remote sensing. MODIS Terra/Aqua systems provide a very useful instrument for regular monitoring and long term studies (2000-) of lake and reservoir conditions (Olmanson et al. 2011, Wang et al. 2012), with algorithms ranging from simple empirical regressions to semi-analytical inversions which have successfully been used to estimate Chl_a concentrations (Kerfoot et al. 2008, Moses et al. 2009, Wang et al. 2011). However, unlike global ocean products, there are no standard Chl_a products in coastal and inland waters, where optically active constituents vary

independently ([IOCCG 2000](#)). Importantly, MODIS Terra/Aqua bands from 412 to 869 nm are often saturated in coastal and inland waters due to elevated atmospheric and water turbidity, as these systems were mainly designed for ocean use with a highly sensitivity and narrow dynamic range ([Hu et al. 2012](#)). For inland waterbodies, novel Chla retrieval approaches must be developed using non-saturating bands present in the land and atmosphere based sensors ([Qi et al. 2014a](#)). In addition, MODIS does not has a 620 nm band, making it difficult to build direct PC algorithms based on radiative transfer ([Kutser et al. 2006](#), [Tao et al. 2017](#)). In recent years, artificial intelligence approaches, neural network models, support vector machine (SVM) algorithms and Empirical Orthogonal Functions (EOF), have been used to estimate of pigment concentration ([Bonansea et al. 2015](#), [Craig et al. 2012](#), [Schiller and Doerffer 2005](#), [Sun et al. 2009](#)). These models are focused on reducing the dimensionality of remotely sensed data and bringing out features that would not normally be evident. They do not directly address the bio-optical properties of the specific phytoplankton pigment, but rather empirically address changes that are due to the variability of the bio-optical properties within a set of multiple images.

Lake Chaohu supports an important commercial fishing industry as well as tourism and recreation activities ([Xu et al. 2005](#)). The western section of Lake Chaohu was, until 2007, the major potable water source for Hefei City (the capital city of Anhui province, China). The eastern lake is still the main drinking-water source for Chaohu City. Due to the increasing occurrence of cyanobacterial blooms in the eastern lake, authorities are looking for new approaches to manage water supplies to this city with nearly 1 million people

(Zhang et al. 2015). The objectives of this study were: 1) to develop and evaluate MODIS-based algorithms to estimate Chla and PC using EOF approaches, and explore potential benefits of EOF analytics under thick aerosol; 2) to derive a satellite series spatial-temporal distributions of Chla, PC and PC:Chla in 2000-2014 and explore their influencing factors; 3) to assess the potential health risk of cyanobacterial blooms in current drinking-water sources and recommend the possible future sites for drinking-water source. While there are a number of studies using MODIS to quantify cyanobacteria, cyanobacteria blooms, and cyanobacteria bloom phenology (Becker et al. 2009, Kutser et al. 2006, Wynne et al. 2013); this is the first study to focus on cyanobacterial dominance and their driving forces over such an extensive dataset.

II. Materials and Methods

2.1 Study area

Lake Chaohu (117.24°–117.90° E, 31.40°–31.72° N) is the fifth-largest freshwater lake of China, with an average water depth of 2.5 m and a surface water area of 770 km². Its residence time is about 150 days in the rainy season and 210 days in the dry season (Tu et al. 1990). Nine rivers contribute 90% of the total water inflow to the lake (Yang et al. 2013), while the Yuxi River outflows from eastern lake area to the Yangtze River (Fig. 1). Before the 1960s, Lake Chaohu was well-known for its scenic beauty and for the importance of its fisheries and lake-related economic activities (Xu 1997). However, the lake has suffered from eutrophication and frequent cyanobacterial blooms in recent decades (Kong et al. 2013, Zhang et al. 2015), due to local rapid population growth and economic development. Nutrient-rich inflows to the west lake from the Nanfei River, Shiwuli River and Pai River which discharge about 10 million tons per year of untreated domestic and industrial wastewater from Hefei City (capital of Anhui Province) (Xu et al. 2005). This has led to an elevated eutrophication of the western lake, where the mean concentrations of TP and TN were significantly higher than these in the eastern lake (Yang et al. 2013). As a result of increasing eutrophication and the reoccurrence of cyanobacterial blooms, the water supply to Hefei City was changed to Dongpu Reservoir from western Lake Chaohu in 2007 (Zhang et al. 2015). Note that the west, central, and east lake segments are hereinafter termed WL, CL, and EL, respectively.

2.2 Data

2.2.1 Field data

Water samples and optical data were collected at 15 sampling stations during seven field investigations between May 2013 and April 2015 in Lake Chaohu (Fig.1 and Table 1), with a total of 259 sampling points collected. Water samples were collected at the surface (~30 cm water depth) with a standard 2-liter polyethylene water-fetching instrument. The samples were stored in cold dark condition before filtering in laboratory conditions.

PC was measured using a spectrofluorophotometer (Shimadzu RF-5301, 620-nm excitation and 647-nm emission) and a reference standard from Sigma Company ([Duan et al. 2012b](#), [Qi et al. 2014b](#)). Chla was measured spectrophotometrically using NASA recommended and community-accepted protocols ([Mueller et al. 2003](#)). Suspended particulate matter (SPM) concentrations were measured gravimetrically on pre-combusted and pre-weighed 47 mm GF/F after drying overnight at 105°C overnight ([Cao et al. 2017](#), [Duan et al. 2012b](#)).

2.2.2 MODIS Data

Cloud free data granules covering the study region between February 2000 and December 2014 were obtained from the U.S. NASA Goddard Space Flight Center (GSFC) (Table S1). Level-0 data were processed using SeaDAS version 7.2 to generate calibrated at-sensor radiance. An initial attempt to use SeaDAS to generate above-water remote-sensing reflectance (R_{rs}) ([Wang and Shi 2007](#)) was unsuccessful due to elevated aerosol

concentrations and sun glint, even after adjusting the processing options (e.g., the default limit of aerosol optical thickness at 869 nm was increased from 0.3 to 0.5, and the default cloud albedo was raised from 2.7% to 4.0%, etc.) (Duan et al. 2014, Feng et al. 2012). The R_{rc} was derived after correction for Rayleigh scattering and gaseous absorption effects (Hu et al. 2004). As the ocean bands were frequently saturated over Lake Chaohu due to the turbid atmospheric and lake conditions; they were not employed in this study. The 250m MODIS bands at 645 nm and 859 nm and the 500 m bands at 469 nm, 555 nm, 1240 nm, 1640nm and 2130 nm cover a higher dynamic range than the ocean bands and, therefore, rarely saturate in turbid waters (Hu et al. 2012). As the 1240 nm, 1640 nm and 2130 nm bands often contain substantial noise due to detector artifacts (Wang and Shi 2007), only four bands at 469, 555, 645, and 859 nm were employed in this study.

2.3 MODIS Chla and PC products

According to past and present field measurements, Lake Chaohu has three general optical conditions: "clean" water, a highly turbid state dominated by elevated concentrations of suspended matter, and a cyanobacteria-bloom-dominated (Tao et al. 2017). Of the three conditions, water with high-suspended matter had a higher R_{rc} compared to clear water areas, but this difference was much smaller than that between these water conditions and bloom-dominated waters. Bloom-dominated reflectance in the near-infrared band (859 nm) showed a high differentiation.

Following earlier studies in waters with high concentrations of suspended matter, we used

FAI=0.02 as the threshold for the pixels of pure cyanobacterial bloom (Hu et al. 2010).

However, three situations arise which reduce the effectiveness of FAI class separation:

water-land boundary effects, bands with striping noise, and small-scale cyanobacterial

blooms. To reduce the misidentification of non-bloom conditions for bloom conditions near

land boundaries, all images were visually inspected; the distribution of the number of pixels

in each scene that were affected by a water-land boundary effect was determined. The bloom

and non-bloom images were classified using the standard far outlier threshold (the average

value plus two standard deviations: 285 pixels or 17.80 km²); among the 1806 scenes of

MODIS images, 1156 scenes with non-bloom (class I) conditions, and 650 scenes with

bloom conditions (class II).

The general approach followed multi-step process (Fig. 2), which began with the Raleigh

correction of MODIS L0 data to determine reflectance R_{rc} . The floating algae index (FAI)

was applied to each scene and the distribution of pixels with FAI>0.02 was derived. Using a

standard far outlier threshold (average value plus two standard deviations), an area threshold

(285 pixels or 17.80 km²) was used to differentiate the non-bloom images (class I) and

bloom (class II) images. If the area of cyanobacterial bloom was smaller than 17.80 km², it

was considered a non-bloom image and Model I was employed. If the bloom area was larger

than this threshold, it was considered to be a bloom image, and Model II was employed. The

input parameters of the Model I and Model 2 were determined by regression of EOF

decomposition values with in situ measured Chla and PC concentrations, respectively.

EOF is used to reduce multi-band reflectance data to uncorrelated and independent variables (i.e., EOF modes) which are then applied to retrieve water quality parameters (Barnes et al. 2014, Craig et al. 2012, Qi et al. 2014a). The development of the EOF algorithms followed three steps: (1) The first step was to normalize the R_{rc} spectra to derive the NR_{rc} data, and perform an EOF analysis (eg. using the princomp function in MATLABTM) on NR_{rc} . The output of the EOF decomposition includes the score vector of each EOF mode; each score vector is a linear composition of the four original bands. The output also includes the load value of each band, namely, the coefficients for the linear combination from the original bands to the score vector of each mode; and the variance contributions that describe the degree of the original band variance explained by each EOF mode. (2) The second step was to use a training set of in-situ samples to implement a linear regression analysis with the score values of EOF modes. The relationship between EOF modes and changes in the concentrations of phytoplankton pigment (Chla or PC) (e.g. using the regress function in MATLABTM) followed:

$$\beta_0 + \beta_1 T_1 + \beta_2 T_2 + \beta_3 T_3 + \beta_4 T_4 = \text{pigment concentration} \quad (1)$$

where T_1 , T_2 , T_3 , and T_4 were the score values of the four modes and (β_{0-4}) were the regression coefficients. (3) The final step was to apply the EOF based Chla or PC algorithms to the MODIS image datasets. More detail are well described in Tao et al. (2017).

2.5 Cyanobacterial risk mapping

A decision tree classification model (Fig. S1) based on Chla and PC:Chla was developed to

assess cyanobacterial risk (Hunter et al. 2009). This approach was inspired by the WHO guidance levels, which uses the concentration of cyanobacterial cells (or an equivalent concentration of Chla) to estimate the level of risk (WHO 2011). However, the WHO guidance levels do not differentiate the actual biomass of cyanobacteria from that of the total phytoplankton biomass (Tyler et al. 2009). To indicate the relative contribution of cyanobacteria to total biomass, several previous studies used a proxy indicator (Duan et al. 2012b, Shi et al. 2015a, Simis et al. 2007), expressed as the ratio of the PC concentration to the Chla concentration. We used this ratio, PC:Chla, to indicate waters with a cyanobacterial dominance .

2.6 Accuracy assessment

The algorithm performance was assessed using four indices, namely the relative root mean square error, unbiased RMSE (URMSE) in relative percentage (100%), mean normalized bias (MNB), and normalized root mean square error (NRMS), defined as:

$$RMSE_{rel} = 100 \sqrt{\frac{1}{n} \sum_{i=1}^n (\varepsilon_i)^2} \quad (2)$$

$$URMSE(\%) = \sqrt{\frac{1}{n} \sum_{i=1}^n \left(\frac{y_i - x_i}{0.5(y_i + x_i)} \right)^2} \times 100\% \quad (3)$$

$$MNB = 100 \text{mean}(\varepsilon_i) \quad (4)$$

$$NRMS = 100 \text{stdev}(\varepsilon_i) \quad (5)$$

where ε_i represents the relative difference between algorithm-retrieved and measurement concentrations for the i^{th} measurement; y is the algorithm result and x is the measurement, and n the sample size. URMSE was used to avoid deviations that cause skewed error distributions. MNB is a measure of the systematic errors, NRMS is a measure of random

238 errors.

III. Results

3.1 Algorithm development and validation

Large spatial and temporal variabilities in Chla and PC were observed during the 7 cruises (Table 1). Chla ranged from 6.85 to 1229.83 $\mu\text{g/L}$, PC ranged from 8.88 to 4807.72 $\mu\text{g/L}$, and PC:Chla varied between 0.09 and 50.39. Spatially, Chla and PC were much higher in WL than those in CL and EL. Temporally, the average Chla and PC were highest in summer (from May to September) while bloom initiation occurred in early spring (April).

The Chla algorithm was developed using 87 data pairs from MODIS and in situ data (half the data set) (Fig. 3a). There was a statistically significant correlation between the EOF-modeled Chla and measured Chla, with a coefficient of determination (R^2) of 0.64 and $\text{RMSE}_{\text{rel}}=70.12\%$. The data were scattered around the 1:1 line, and the Chla algorithm overestimates Chla with $\text{MNB}=19.17\%$ and $\text{NRMS}=67.45\%$. The PC algorithm showed similar performance with $R^2=0.60$, and lower uncertainties in all statistical measures ($\text{RMSE}_{\text{rel}}=38.33\%$, $\text{MNB}=26.98\%$, $\text{NRMS}=73.50\%$) (Fig. 3c).

The performance of the Chla and PC algorithms was assessed using the remaining 93 datasets, and the results showed significant correlations between modelled and *in situ* concentrations. For Chla, $R^2=0.40$, $\text{RMSE}_{\text{rel}}=58.38\%$, $\text{MNB}=18.68\%$, and $\text{NRMS}=62.74\%$ (Fig. 3b); while for PC, $R^2=0.40$, $\text{RMSE}_{\text{rel}}=57.96\%$, $\text{MNB}=38.11\%$, and $\text{NRMS}=69.92\%$ (Fig. 3d). The performance of the algorithm was acceptable considering that four land bands

and a partial atmospheric correction were used. Importantly, the error bars of Chla and PC also showed reasonable results (Figs. 3e and 3f). Additionally, the retrieved PC patterns from MODIS are spatially consistent in two conditions (Bloom and Non-bloom) with MERIS PCI products (Tao et al. 2017), which have provided reliable PC estimations in other inland water bodies (Qi et al. 2014b).

3.2 Long-term trend and variability

The EOF-based algorithms were used to derive a long-term Chla and PC values from available MODIS data, and these values were integrated with annual and monthly means.

3.2.1 Chla

The seasonal mean EOF-derived satellite Chla showed significant spatial and temporal variability (Fig. S2). In general, Chla was highest in the western lake (WL) compared to the central and eastern lake areas (CL and EL). The WL is highly eutrophic due to the high degree of urban wastewater brought to the lake through the Nanfei, Shiwuli and Pai rivers (Fig. 1), which discharge millions of tons per year of wastewater from Hefei City. CL showed the lower Chla as it receives the much clearer waters from the Hangbu, Baishishan and Zhao rivers, which account for nearly half of the total freshwater input into the whole lake. The annual mean Chla of WL was consistently higher than that of CL and EL, and ranged from $21.16 \mu\text{gL}^{-1}$ in 2004 to $75.65 \mu\text{gL}^{-1}$ in 2012, with a long-term mean of $36.97 \pm 16.19 \mu\text{gL}^{-1}$ for the 15-year period (Fig. 4a). For EL, Chla ranged from $19.49 \mu\text{gL}^{-1}$ in 2001 to $44.18 \mu\text{gL}^{-1}$ in 2012 (mean = $31.01 \pm 8.42 \mu\text{gL}^{-1}$). Chla in CL was the lowest, ranging

between $16.34 \mu\text{gL}^{-1}$ in 2005 and $39.63 \mu\text{gL}^{-1}$ in 2010 (mean = $27.19 \pm 7.42 \mu\text{gL}^{-1}$). Of the three lake segments, WL showed the highest inter-annual variability, with a 15-year standard deviation (SD) of $16.19 \mu\text{gL}^{-1}$, and followed by EL ($8.42 \mu\text{gL}^{-1}$) and CL ($7.42 \mu\text{gL}^{-1}$). All three lake segments exhibited similar temporal patterns with increasing Chla trend, and Chla in each segment between 2000 and 2006 was significantly lower than between 2007 and 2014. Chla showed a noticeable decrease in 2014 in EL. In general, years with large positive anomalies included 2007 and 2014, while years with large negative anomalies included 2000 and 2006.

Seasonal dynamics showed multiple Chla maxima in September (CL and EL) and October (WL) and annual minimum in April in the entire lake (Figs. S3 and 5a). All three lake segments in February showed a second Chla peak due to high amount of Bacillariophytes present in early spring (no similar PC peak) (Deng et al. 2007). WL showed the highest Chla through the seasonal cycle (21.96 - $63.63 \mu\text{gL}^{-1}$), followed by EL (19.26 - $54.95 \mu\text{gL}^{-1}$) and CL (17.31 - $51.87 \mu\text{gL}^{-1}$).

3.2.2 PC

Compared with Chla, estimated PC showed more significant spatial variability (Figs. S4 and S5). Annual mean PC was consistently high in WL with peaks in 2000, 2001 and 2009, and relatively low in CL and EL throughout the study period (2000-2014) (Fig. 4b). High PC values further extended to the CL and EL in 2011. The long-term mean in WL was $62.02 \pm 19.94 \mu\text{gL}^{-1}$, while long-term means were $17.01 \pm 6.10 \mu\text{gL}^{-1}$ and $19.36 \pm 4.85 \mu\text{gL}^{-1}$ in

CL and EL, respectively.

Seasonal distributions showed higher PC observed in summer and autumn (June-October) (Figs. 5b. and S4). Mean PC reached annual maxima in August (EL) or September (WL and CL). Similar to the annual mean statistics, WL showed the highest mean PC through the seasonal cycle ($66.27 \pm 52.46 \mu\text{gL}^{-1}$); in contrast to CL ($18.16 \pm 8.81 \mu\text{gL}^{-1}$) and EL ($21.68 \pm 10.80 \mu\text{gL}^{-1}$). For all three lake segments, seasonal variability overwhelmed inter-annual variability.

3.2.3 PC:Chla

PC:Chla distributions, derived from Chla and PC products mentioned above showed large spatial and temporal variability (Figs. 6 and 7). From 2000-2014, PC:Chla showed a general decreasing trend in WL with significant inter-annual variability (Fig. 4c). In WL, PC:Chla ranged from 0.67 in 2010 to 2.58 in 2001, with an average value of 1.72 ± 0.56 . Annual mean PC:Chla in CL and EL were lower, with long-term means of 0.62 ± 0.24 and 0.64 ± 0.21 , respectively. Similar the Chla and PC patterns, monthly PC:Chla also showed significant seasonality, but with highest PC:Chla in the late spring and summer (April-August) (Figs. 5c and 7). This seasonal variation confirmed previous field surveys on the dominance of green algae and diatom in the spring, and a shift to cyanobacteria in summer contributing 70%-90% to the total phytoplankton biomass (Deng et al. 2007, Li et al. 2015).

IV. Discussion

4.1 Algorithm performance

There are several studies for estimating pigments such as Chla and PC. For Chla, the ratio of near-infrared (around 700-710nm) to red (around 665-685nm) reflectance, to highlight the differences between the absorption maximum and minimum of pigment and water, has been successfully applied to a wide range of turbid water bodies ([Dekker 1993](#), [Mittenzwey et al. 1992](#)). This method depends on empirical linear regression to predict Chla of lakes water. Using similar bands ratio but based on radiative transfer modelling ([Gordon et al. 1975](#)), Gons developed a semi-analytical algorithm for Chla retrieval ([Gons 1999](#)). Furthermore, a three-band model was also developed to estimate Chla concentration ([Dall'Olmo et al. 2003](#)), and the two band ratio model was regarded as a special case of the three-band model ([Gitelson et al. 2008](#)). Similar to Chla, PC can be detected based on the absorption feature around 620 nm ([Bryant 1994](#)), and current algorithms are based on the quantification of the reflectance trough at this region in remotely sensed data ([Ruiz-Verdu et al. 2008](#), [Simis et al. 2007](#)). However, these algorithms developed in inland waters are designed using field measured remote sensing reflectance (R_{rs}), and depend strongly on the absolute accuracy of satellite-based R_{rs} ([Duan et al. 2012a](#), [Le et al. 2013](#)). In fact, accurate cyanobacterial pigments retrievals, especially for PC, from satellite measurements in inland waters have been notoriously difficult to develop due to the complex and highly variable nature of these waters.

MODIS was designed for oceanic waters and easily saturated over turbid waters. Even without saturation, the requirements of the atmospheric correction on aerosol optical thickness (<0.3 at 859 nm) make valid MODIS R_{rs} retrievals extremely sparse in those waters (Qi et al. 2014a). This would produce the limited number of MODIS bands, together with the large uncertainties in the full atmospheric correction over turbid waters. Given the difficulties in atmospheric corrections and the nature of the optical variability in Lake Chaohu, the EOF approach provided reasonable results to derive long-term cyanobacteria distribution information. This is especially true when considering the Chla and PC patterns are reasonable (Figs. S2-S5) and low sensitivity to high SPM concentrations contained and atmospheric aerosols perturbations (Fig. S6). The three RGB images in three subsequent days on 5 and 7 January 2007 were generated from data collected under different conditions (Figs. S6a- S6c). Figs. S6a- S6b showed an example where significant turbidity changes occurred in most of the lake waters in two subsequent days on 6 and 7 January 2007, yet their corresponding PC (Figs. S6d- S6e) and Chla images (Fig. S6) showed tolerance to such significant turbidity changes, as revealed by the very similar PC and Chla distribution patterns for pixels both impacted and not impacted by the turbid changes. Fig. S6c shows another example where the PC and Chla EOF algorithms are both insensitive to perturbations due to thick aerosols. Despite the whole lake experience significant aerosols, yet the PC (Fig. S6f) and Chla (Fig. S6i) values under this condition were similar to those derived under non-thick aerosols from another two days (Figs. S6d- S6e, S6g- S6h). This might be due to the spectral normalization which partially remove the sediments and aerosol effects while retaining most the spectral information; of the four spectral bands, three visible

bands contain information from cyanobacterial pigments. This has also been confirmed in Lake Taihu and Tampa bay (Le et al. 2013, Qi et al. 2014a).

It is important note that the use of EOF and single-lake training provides a solution for one lake, and possibly nearby lakes. The solution is not likely to transfer to other locations well, and the two algorithms may not be able to move directly to other lakes. Given that the lake is of high importance for drinking water supply, and given that the method used to 'train' the model is transferable with the requirement for additional field work, the approach will nevertheless be of interest to water management authorities elsewhere.

4.2 Cyanobacterial dominance and its driving factors

Cyanobacterial dominance in anthropogenically impacted eutrophic lakes is an increasing problem that impacts ecosystem integrity and human and animal health (Downing et al. 2001). Understanding the cause of cyanobacterial dominance has been a focal point of classical and contemporary limnological research (Havens et al. 2003). The established long-term Chla, PC concentrations and their ratio (Figs. 8a-8c) provide an opportunity to further evaluate the driving forces that control cyanobacterial biomass and potential relation with physical variability in temperature and nutrients.

Since the earliest studies of phytoplankton ecology, nutrients have been invoked as one of the variables controlling phytoplankton community structure and a predictor of the dominance of cyanobacteria. However, the annual mean Chla and PC in the three lake

segments do not demonstrate significant positive correlations with annual mean TN and TP (Fig. 4). In fact, TN and TP showed a general decreasing trend throughout the 15 years (Figs. 8d-8e); in contrast, Chla and PC increased, in particular in the years after 2009. The 15-year time-series between Chla and PC and nutrients did not show significant correlations (Fig. 8). Generally, nutrient enrichment is a prerequisite to cyanobacterial dominance and bloom formation, and numerous bioassay experiments have demonstrated that phosphorus and at times nitrogen can act as the limiting resource (Droop 1974, Tilman et al. 1982, Xu et al. 2010). This is also confirmed by that the high Chla and PC patterns primarily occupied in WL and tended to decrease from the western to the eastern region in Lake Chaohu (Figs. 5 and 6), consistent with the distribution of nutrients determined from field samples (Figs. 8d-8f). However, the role of nutrient concentrations in controlling cyanobacteria dynamics might be limited due to elevated concentrations and low inter-annual variation, and they are likely in excess of algal growth demand. Note that the annual minimum nutrient concentrations (TN: 1.50 mg/L in 2007; TP: 0.10 mg/L in 2010) during 2000-2014 in Lake Chaohu exceeded cyanobacteria growth requirements (TN: 1.26 mg/L, TP: 0.082 mg/L) recommended to maintain bloom-free conditions in Lake Taihu (Xu et al. 2014), which is at a similar latitude and is dominated by *Microcystis* blooms. This explains why cyanobacterial blooms can still thrive for much of the year in Lake Chaohu, despite the efforts being undertaken to control nutrient loading.

Compared with TN or TP, the TN:TP ratio has been shown to impact the phytoplankton species composition, where low N:P favours the production of cyanobacterial blooms (Liu et

al. 2011, Tilman et al. 1982). When nutrients are not limiting, the molar elemental ratio (Redfield ratio) N:P in most phytoplankton is 16:1 (Redfield 1934). A TN:TP ratio of 29:1 differentiates between lakes with cyanobacterial dominance (TN:TP<29:1 by mass) and lakes without such dominance (TN:TP>29:1) in temperate lakes (Smith 1983). Subsequent multi-lake surveys and controlled experiments have generally supported this hypothesis (Havens et al. 2003). TN:TP rarely went above 29:1 in CL (4 months) and EL (6 months) in 168 months between 2001 and 2014; while this threshold was surpassed in 18 months of 84 months between 2008 and 2014. The nutrient data in WL was only collected during 2008-2014. Using this threshold, all PC:Chla data in WL during 2008-2014 were reorganized and separated into two categories. In months with TN:TP larger than 29:1, the corresponding average PC:Chla was 0.64; while months below 29:1, averaged 1.91 PC:Chla (Figs. 8c and 8f). Note that the annual relative cyanobacteria to total phytoplankton biomass (PC:Chla) (Figs. 4c and 6) in three lake segments especially WL showed a slight decreasing trend in recent years, compared with an increasing TN:TP value (Fig. 4d); and they displayed a significant negative correlation in the entire lake ($r = -0.39$, $p < 0.5$). The mechanism proposed to link cyanobacterial dominance to a low TN:TP ratio is that all species of cyanobacteria are better able to compete for nitrogen than other phytoplankton when N is scarce. Therefore, when excessive P loading creates a surplus supply of phosphorus, N becomes relatively scarce and cyanobacteria are predicted to become dominant (Smith 1983).

Seasonal succession in the phytoplankton assemblages has been observed in many eutrophic

lakes, and temperature has been associated as an important factor responsible for the seasonal shift of phytoplankton community (Elliott et al. 2006). Field surveys showed that there was nearly 200 phytoplankton species mainly including Chlorophytes (101 species), Cyanophytes (46 species) and Bacillariophytes (28 species) in Lake Chaohu (Deng et al. 2007), and the dominated group shifted from green algae and diatoms in the spring to cyanobacteria in the summer and autumn (Deng et al. 2007, Li et al. 2015). This is consistent with our monthly Chla, PC and PC:Chla values (Figs. 5a-5c and 7). Chla reached its first peak in February (Fig.5a) due to quick increasing of diatom (Bacillariophytes), which was a superior competitor at temperatures below 15 °C (Tilman et al. 1986). PC and PC:Chla showed their first peaks during summer between June and September with increasing temperature (Figs. 5b and 5c). It has been reported that diatoms dominated under conditions of low water temperature in Lake Chaohu (Deng et al. 2007). However, cyanobacteria generally grow better at higher temperatures than other phytoplankton species such as diatoms and green algae, and this gives cyanobacteria a competitive advantage at elevated temperatures (Elliott et al. 2006, Joehnk et al. 2008, Paerl and Huisman 2008). Fig. 9 shows that the monthly mean temperatures were well correlated with PC ($r = 0.71$, Fig. 9b), but low with Chla or PC:Chla ($r < 0.22$, Figs. 9a and 9c). This is because cyanobacteria contribute a large proportion, 90% or more of the total phytoplankton biomass, at higher temperatures, in particular in the summer (Li et al. 2015). Additionally, there are two cyanobacteria taxa in Lake Chaohu, *Anabaena* dominance in spring was overcome by increasing *Microcystis* dominance in summer (Yu et al. 2014, Zhang et al. 2016). This will also result in increasing PC concentrations with increasing temperature, and large seasonal

variations of Chla and PC:Chla.

Factors causing the dominance of a phytoplankton group are often difficult to reveal because several interacting factors including hydrodynamic effects are usually involved which are not necessarily the same in different environments (Dokulil and Teubner 2000). Nutrients and temperature are generally regarded as the most important factors affecting phytoplankton community succession, but their relative importance depends on the lake and its location, changes in (wind-driven) turbulence, light availability, and nutrient balance. It has been reported that many diatoms are superior phosphorus competitors and inferior competitors for light and nitrogen at temperatures below 15 °C, whereas many cyanophytes species are superior nitrogen and inferior phosphorous competitors, showing their competitive potential at temperatures above 20 °C (Deng et al. 2007, Tilman et al. 1986). However, when nutrient concentrations are higher than cyanobacteria growth requirement, warm water would increase activity rates of cyanobacteria and enhance the probability of cyanobacterial dominance (Duan et al. 2009, Liu et al. 2011, Wagner and Adrian 2009). A recent study of cyanobacterial dominance based on 1000 US lakes demonstrates that the relative importance of these two factors was dependent on lake trophic state: Nutrients play a larger role in oligotrophic lakes, while temperature is more important in mesotrophic lakes; Only eutrophic and hyper-eutrophic lakes exhibit a significant interaction between nutrients and temperature (Rigosi et al. 2014). In Lake Chaohu, nutrient concentrations are so high that cyanobacteria growth is mainly controlled by temperature and light availability. The incidence of cyanobacteria blooms will certainly increase under future climate warming, if

there is no significant nutrient reduction.

4.3 Implication for safety evaluation in drinking-water source

Harmful cyanobacterial blooms pose a threat to freshwater ecosystems used for drinking-water supply due to the production of cyanotoxins such as microcystins (MCs), which act as a protein phosphatase inhibitors and tumour promoters, causing acute and chronic poisoning in humans and animals, particularly liver injury (Falconer et al. 1983, Paerl and Huisman 2009). MCs are produced by several cyanobacterial genera including *Microcystis* and *Anabaena* (Chorus and Bartram 1999), the dominant species in Lake Chaohu (Yu et al. 2014, Zhang et al. 2016). As a water shortage city, Chaohu City with nearly 1 million people has only one drinking-water source in the EL section of Lake Chaohu (Fig.1). In fact, Hefei City used to rely on the WL section as its principal drinking-water source until it was forced to find an alternative source due to heavy cyanobacterial blooms around 2007.

Previous efforts have shown the effectiveness of using a decision tree for cyanobacterial risk monitoring and assessment (Carvalho et al. 2011, Hunter et al. 2009, Shi et al. 2015a, Tyler et al. 2009). Using the present EOF based approach on data from Lake Chaohu during 2000-2014, spatial and inter-annual variations of cyanobacterial risk indicated a high heterogeneity (Figs. 10 and 11). Most of the lake remains at low and no risk, only the WL occasionally displayed a medium risk in the years 2004-2009 and 2011-2014. No high risk years were observed. As expected, the WL showed the highest occurrence of low and

medium risk rank in the entire lake. The EL was dominated by low and no risk while the conditions of the CL were usually no risk. The years 2000, 2001, 2003, 2005, 2009 and 2011 showed the largest areas of low risk. Seasonal distribution confirmed an increased risk during the months with the highest temperature (July-September), and a reduced risk in the winter. It's also worthy noticing that the largest spatial variability was revealed in September, while WL with medium risk rank and CL and EL were both with no risk. This may be the result the prevailing southeast wind in this period that increased the transport of surface algae to the west. In such conditions, re-accessing the WL for domestic water supply to Hefei City remains problematic.

To meet the current drinking-water requirement for Chaohu City, the distribution of past risk conditions around the source was used to create a distributed water quality decision matrix (WQDM, Table 2). Using annual monthly mean Chla and PC in 5 km buffer zones around the drinking-water source in EL derived from MODIS (2000-2014), WQDM was derived first using the threshold Chla and PC:Chla values obtained from the decision tree (Fig. S1). Then these values were derived from satellite data products and a WQDM was generated using these values. Results indicated that there were generally low risks, and occasionally medium risks, while none risk occurred between January and March during winter. This present a significant problem for the drinking water supply to Chaohu City with potential increases in human health related risks.

One possible way to remediate the problem would be to move the drinking-water source to

another site in Lake Chaohu. By considering the WQDM, based on areas with the highest frequency of no risk, it's possible to identify the most appropriate water intake areas of the lake, considering the past 14 years of data (Figs.12a-12d). Several areas in the CL were good candidates, with 60% or more frequency with no risk (Fig.12a); however, with a 30% frequency of low risk (Fig.12b). The closest of these areas was almost 30 km from Chaohu city. There was no location with 100% frequency no risk (Fig.12d).

Another option would be supplement water treatment during the periods of the year that are most prone to increased risk in the area of the domestic water intake in the EL. Focused water treatment in this period to remove MCs would reduce risk for the population of Chaohu city while not incurring the costs of year round treatment. In general, there were low and occasionally medium risks in the 5 km buffer zones around the present day drinking-water source area, with no risk conditions never occurring only between January and March (Table 2). As low risk means the surface water contained $5\sim 25\ \mu\text{gL}^{-1}$ PC and $10\sim 50\ \mu\text{gL}^{-1}$ Chla (Fig. S1), this translated to an equivalent to $0.80\sim 3.98\ \mu\text{gL}^{-1}$ MCs (Shi et al. 2015b). This is higher than the threshold ($1\ \mu\text{gL}^{-1}$) suggested by WHO for drinking water (Otten et al. 2012).

The combination of identifiable thresholds that lead to increased risk of compromised water supplies and regular monitoring using remote sensing provides a new tool for the management of lakes used for domestic water supplies. It is also worth mentioning that present satellite constellations would allow for relatively rapid detection of changes in lake

537 state, allowing for early warning and mitigation of the drinking water quality during intake.
538 By building spatially explicit historical datasets, it possible to estimate the relative risk of
539 positioning (or repositioning) water intakes. When cost or infrastructure limitations prohibit
540 the access to low risk lake areas, temporally focused actions to improve treatment (or
541 increased monitoring) with respect to local conditions can be made. The ultimate solution
542 will be to reduce nutrient loads of surface waters, but complex in-lake processes and nutrient
543 storage do not allow for simple linear solutions.

V. Conclusions

In this study, we used an EOF approach to estimate the concentrations of Chla and PC from MODIS in Lake Chaohu. Based on 1806 MODIS images acquired from 2000 to 2014, we found that PC:Chla ratio has a great potential to detect the cyanobacterial dominance, and the nutrient and climate conditions favor this dominance. Additionally, long-term cyanobacterial risk in Lake Chaohu was assessed with a Water Quality Decision Matrix based on MODIS Chla and PC products. The results provide new insights that could assist authorities in the identification of possible intake areas, as well as specific months when higher frequency monitoring and more intense water treatment would be required using the present intake area in Lake Chaohu. This study demonstrates that remotely sensed cyanobacterial risk mapping provides a new tool for management programs for this and similar lakes and reservoirs.

ACKNOWLEDGEMENTS

The authors would like to thank all participants and voluntary contributors (Jinghui Wu, Xiaoyu Pang, Meishen Yi, Jing Li and Kun Xue [Nanjing Institute of Geography and Limnology, Chinese Academy of Sciences: NIGLAS]). Thanks also to Dr. Chuanmin Hu [University of South Florida: USF] and Min Zhang [NIGLAS] for their valuable suggestions and comments. Financial support was provided by the Provincial Natural Science Foundation of Jiangsu of China (BK20160049), National Natural Science Foundation of China (41671358, 41431176), Youth Innovation Promotion Association of CAS (2012238), National Key Research and Development Program of China (2016YFB0501501), and NIGLAS Cross-functional Innovation Teams (NIGLAS2016TD01). Collaboration support was provided by Dragon 4 Cooperation Program project 32442.

References

- Barnes, B.B., Hu, C., Cannizzaro, J.P., Craig, S.E., Hallock, P., Jones, D.L., Lehrter, J.C., Melo, N., Schaeffer, B.A. and Zepp, R. (2014) Estimation of diffuse attenuation of ultraviolet light in optically shallow Florida Keys waters from MODIS measurements. *Remote Sensing of Environment* 140, 519-532.
- Becker, R.H., Sultan, M.I., Boyer, G.L., Twiss, M.R. and Konopko, E. (2009) Mapping cyanobacterial blooms in the Great Lakes using MODIS. *Journal of Great Lakes Research* 35(3), 447-453.
- Bonansea, M., Rodriguez, M.C., Pinotti, L. and Ferrero, S. (2015) Using multi-temporal Landsat imagery and linear mixed models for assessing water quality parameters in Río Tercero reservoir (Argentina). *Remote Sensing of Environment* 158, 28-41.
- Bresciani, M., Adamo, M., De Carolis, G., Matta, E., Pasquariello, G., Vaičiūtė, D. and Giardino, C. (2014) Monitoring blooms and surface accumulation of cyanobacteria in the Curonian Lagoon by combining MERIS and ASAR data. *Remote Sensing of Environment* 146(0), 124-135.
- Bryant, D. (1994) *The Molecular Biology of Cyanobacteria*, Kluwer Academic Publishers.
- Cao, Z., Duan, H., Feng, L., Ma, R. and Xue, K. (2017) Climate- and human-induced changes in suspended particulate matter over Lake Hongze on short and long timescales. *Remote Sensing of Environment* 192, 98-113.
- Carvalho, L., Miller, C.A., Scott, E.M., Codd, G.A., Davies, P.S. and Tyler, A.N. (2011) Cyanobacterial blooms: Statistical models describing risk factors for national-scale lake assessment and lake management. *Science of the Total Environment* 409(24), 5353-5358.
- Chorus, I. and Bartram, J. (1999) *Toxic cyanobacteria in water: a guide to their public health*

- consequences, monitoring, and management, Taylor & Francis.
- Craig, S.E., Jones, C.T., Li, W.K.W., Lazin, G., Horne, E., Caverhill, C. and Cullen, J.J. (2012) Deriving optical metrics of coastal phytoplankton biomass from ocean colour. *Remote Sensing of Environment* 119(0), 72-83.
- Dall'Olmo, G., Gitelson, A.A. and Rundquist, D.C. (2003) Towards a unified approach for remote estimation of chlorophyll-a in both terrestrial vegetation and turbid productive waters. *Geophysical Research Letters* 30(18), 1938.
- Dekker, A.G. (1993) Detection of optical water quality parameters for eutrophic waters by high resolution remote sensing, Free University The Netherlands.
- Deng, D.-G., Xie, P., Zhou, Q., Yang, H. and Guo, L.-G. (2007) Studies on Temporal and Spatial Variations of Phytoplankton in Lake Chaohu. *Journal of Integrative Plant Biology* 49(4), 409-418.
- Dokulil, M.T. and Teubner, K. (2000) Cyanobacterial dominance in lakes. *Hydrobiologia* 438(1-3), 1-12.
- Downing, J.A., Watson, S.B. and McCauley, E. (2001) Predicting Cyanobacteria dominance in lakes. *Canadian Journal of Fisheries and Aquatic Sciences* 58(10), 1905-1908.
- Droop, M. (1974) The nutrient status of algal cells in continuous culture. *Journal of the Marine Biological Association of the United Kingdom* 54(04), 825-855.
- Duan, H., Feng, L., Ma, R., Zhang, Y. and Loiselle, S.A. (2014) Variability of particulate organic carbon in inland waters observed from MODIS Aqua imagery. *Environmental Research Letters* 9(8), 084011.
- Duan, H., Ma, R. and Hu, C. (2012a) Evaluation of remote sensing algorithms for cyanobacterial pigment retrievals during spring bloom formation in several lakes of East China. *Remote Sensing of*

- 611 Environment 126, 126-135.
- 612 Duan, H.T., Ma, R.H. and Hu, C.M. (2012b) Evaluation of remote sensing algorithms for
 613 cyanobacterial pigment retrievals during spring bloom formation in several lakes of East China.
 614 Remote Sensing of Environment 126, 126-135.
- 615 Duan, H.T., Ma, R.H., Xu, X.F., Kong, F.X., Zhang, S.X., Kong, W.J., Hao, J.Y. and Shang, L.L.
 616 (2009) Two-Decade Reconstruction of Algal Blooms in China's Lake Taihu. Environmental Science
 617 & Technology 43(10), 3522-3528.
- 618 Elliott, J., Jones, I. and Thackeray, S. (2006) Testing the sensitivity of phytoplankton communities to
 619 changes in water temperature and nutrient load, in a temperate lake. Hydrobiologia 559(1), 401-411.
- 620 Falconer, I., Beresford, A. and Runnegar, M.T. (1983) Evidence of liver damage by toxin from a
 621 bloom of the blue-green alga, *Microcystis aeruginosa*. The Medical Journal of Australia 1(11),
 622 511-514.
- 623 Falconer, I.R. and Humpage, A.R. (2005) Health risk assessment of cyanobacterial (blue-green algal)
 624 toxins in drinking water. International Journal of Environmental Research and Public Health 2(1),
 625 43-50.
- 626 Feng, L., Hu, C., Chen, X., Tian, L. and Chen, L. (2012) Human induced turbidity changes in Poyang
 627 Lake between 2000 and 2010: Observations from MODIS. J. Geophys. Res. 117(C7), C07006.
- 628 Gitelson, A.A., Dall'Olmo, G., Moses, W., Rundquist, D.C., Barrow, T., Fisher, T.R., Gurlin, D. and
 629 Holz, J. (2008) A simple semi-analytical model for remote estimation of chlorophyll-a in turbid
 630 waters: Validation. Remote Sensing of Environment 112(9), 3582-3593.
- 631 Gons, H.J. (1999) Optical teledetection of chlorophyll a in turbid inland waters. Environmental
 632 Science & Technology 33(7), 1127-1132.

- 633 Gordon, H.R., Brown, O.B. and Jacobs, M.M. (1975) Computed Relationships between Inherent and
 634 Apparent Optical-Properties of a Flat Homogeneous Ocean. *Applied Optics* 14(2), 417-427.
- 635 Havens, K.E., James, R.T., East, T.L. and Smith, V.H. (2003) N:P ratios, light limitation, and
 636 cyanobacterial dominance in a subtropical lake impacted by non-point source nutrient pollution.
 637 *Environmental Pollution* 122(3), 379-390.
- 638 Hu, C., Chen, Z., Clayton, T.D., Swarzenski, P., Brock, J.C. and Muller-Karger, F.E. (2004)
 639 Assessment of estuarine water-quality indicators using MODIS medium-resolution bands: Initial
 640 results from Tampa Bay, FL. *Remote Sensing of Environment* 93(3), 423-441.
- 641 Hu, C., Feng, L., Lee, Z., Davis, C.O., Mannino, A., McClain, C.R. and Franz, B.A. (2012) Dynamic
 642 range and sensitivity requirements of satellite ocean color sensors: learning from the past. *Applied*
 643 *Optics* 51(25), 6045-6062.
- 644 Hu, C., Lee, Z., Ma, R., Yu, K., Li, D. and Shang, S. (2010) Moderate Resolution Imaging
 645 Spectroradiometer (MODIS) observations of cyanobacteria blooms in Taihu Lake, China. *Journal of*
 646 *Geophysical Research-Oceans* 115(C4), C04002.
- 647 Hunter, P.D., Tyler, A.N., Carvalho, L., Codd, G.A. and Maberly, S.C. (2010) Hyperspectral remote
 648 sensing of cyanobacterial pigments as indicators for cell populations and toxins in eutrophic lakes.
 649 *Remote Sensing of Environment* 114(11), 2705-2718.
- 650 Hunter, P.D., Tyler, A.N., Gilvear, D.J. and Willby, N.J. (2009) Using Remote Sensing to Aid the
 651 Assessment of Human Health Risks from Blooms of Potentially Toxic Cyanobacteria. *Environmental*
 652 *Science & Technology* 43(7), 2627-2633.
- 653 IOCCG (2000) Remote Sensing of Ocean Colour in Coastal, and Other Optically-Complex, Waters.
 654 Stuart, V. (ed).

- 655 Joehnk, K.D., Huisman, J., Sharples, J., Sommeijer, B., Visser, P.M. and Stroom, J.M. (2008) Summer
656 heatwaves promote blooms of harmful cyanobacteria. *Global Change Biology* 14(3), 495-512.
- 657 Kerfoot, W.C., Budd, J.W., Green, S.A., Cotner, J.B., Biddanda, B.A., Schwab, D.J. and Vanderploeg,
658 H.A. (2008) Doughnut in the desert: Late-winter production pulse in southern Lake Michigan.
659 *Limnology and Oceanography* 53(2), 589-604.
- 660 Kong, X.-Z., Jørgensen, S.E., He, W., Qin, N. and Xu, F.-L. (2013) Predicting the restoration effects
661 by a structural dynamic approach in Lake Chaohu, China. *Ecological Modelling* 266, 73-85.
- 662 Kutser, T., Metsamaa, L., Strombeck, N. and Vahtmae, E. (2006) Monitoring cyanobacterial blooms
663 by satellite remote sensing. *Estuarine Coastal and Shelf Science* 67(1-2), 303-312.
- 664 Le, C.F., Hu, C.M., English, D., Cannizzaro, J., Chen, Z.G., Feng, L., Boler, R. and Kovach, C. (2013)
665 Towards a long-term chlorophyll-a data record in a turbid estuary using MODIS observations.
666 *Progress in Oceanography* 109, 90-103.
- 667 Li, J., Cui, K., Lu, W., Chen, Y. and Jiang, Y. (2015) Community dynamics of spring-summer
668 plankton in Lake Chaohu. *Acta Hydrobiologica Sinica* 39(1), 185-192.
- 669 Liu, X., Lu, X.H. and Chen, Y.W. (2011) The effects of temperature and nutrient ratios on *Microcystis*
670 blooms in Lake Taihu, China: An 11-year investigation. *Harmful Algae* 10(3), 337-343.
- 671 Mittenzwey, K.H., Ullrich, S., Gitelson, A. and Kondratiev, K. (1992) Determination of chlorophyll a
672 of inland waters on the basis of spectral reflectance. *Limnology and Oceanography* 37(1), 147-149.
- 673 Morel, A. and Prieur, L. (1977) Analysis of variations in ocean color. *Limnology and Oceanography*
674 22(4), 709-722.
- 675 Moses, W.J., Gitelson, A.A., Berdnikov, S. and Povazhnyy, V. (2009) Estimation of chlorophyll-a
676 concentration in case II waters using MODIS and MERIS data-successes and challenges.

- 677 Environmental Research Letters 4(4), -.
- 678 Mueller, J., Bidigare, R., Trees, C., Dore, J., Karl, D. and Van Heukelem, L. (2003) Biogeochemical
679 and bio-optical measurements and data analysis protocols: ocean optics protocols for satellite ocean
680 color sensor validation. Revision 4, Vol. 2. NASA/TM-2003 21621, 39-64.
- 681 O'Neil, J.M., Davis, T.W., Burford, M.A. and Gobler, C.J. (2012) The rise of harmful cyanobacteria
682 blooms: The potential roles of eutrophication and climate change. Harmful Algae 14(0), 313-334.
- 683 Olmanson, L.G., Brezonik, P.L. and Bauer, M.E. (2011) Evaluation of medium to low resolution
684 satellite imagery for regional lake water quality assessments. Water Resour. Res. 47(9), W09515.
- 685 Otten, T.G., Xu, H., Qin, B., Zhu, G. and Paerl, H.W. (2012) Spatiotemporal Patterns and
686 Ecophysiology of Toxigenic Microcystis Blooms in Lake Taihu, China: Implications for Water
687 Quality Management. Environmental Science & Technology 46(6), 3480-3488.
- 688 Paerl, H.W. and Huisman, J. (2008) Climate - Blooms like it hot. Science 320(5872), 57-58.
- 689 Paerl, H.W. and Huisman, J. (2009) Climate change: a catalyst for global expansion of harmful
690 cyanobacterial blooms. Environmental Microbiology Reports 1(1), 27-37.
- 691 Paerl, H.W., Xu, H., McCarthy, M.J., Zhu, G., Qin, B., Li, Y. and Gardner, W.S. (2011) Controlling
692 harmful cyanobacterial blooms in a hyper-eutrophic lake (Lake Taihu, China): The need for a dual
693 nutrient (N & P) management strategy. Water Research 45(5), 1973-1983.
- 694 Qi, L., Hu, C., Duan, H., Barnes, B.B. and Ma, R. (2014a) An EOF-Based Algorithm to Estimate
695 Chlorophyll a Concentrations in Taihu Lake from MODIS Land-Band Measurements: Implications
696 for Near Real-Time Applications and Forecasting Models. Remote Sensing 6(11), 10694-10715.
- 697 Qi, L., Hu, C., Duan, H., Cannizzaro, J. and Ma, R. (2014b) A novel MERIS algorithm to derive
698 cyanobacterial phycocyanin pigment concentrations in a eutrophic lake: Theoretical basis and

- 699 practical considerations. *Remote Sensing of Environment* 154, 298-317.
- 700 Redfield, A.C. (1934) On the proportions of organic derivatives in sea water and their relation to the
701 composition of plankton, university press of liverpool James Johnstone memorial volume.
- 702 Rigosi, A., Carey, C.C., Ibelings, B.W. and Brookes, J.D. (2014) The interaction between climate
703 warming and eutrophication to promote cyanobacteria is dependent on trophic state and varies among
704 taxa. *Limnology and Oceanography* 59(1), 99-114.
- 705 Ruiz-Verdu, A., Simis, S.G.H., de Hoyos, C., Gons, H.J. and Pena-Martinez, R. (2008) An evaluation
706 of algorithms for the remote sensing of cyanobacterial biomass. *Remote Sensing of Environment*
707 112(11), 3996-4008.
- 708 Schiller, H. and Doerffer, R. (2005) Improved determination of coastal water constituent
709 concentrations from MERIS data. *Ieee Transactions on Geoscience and Remote Sensing* 43(7),
710 1585-1591.
- 711 Schneider, S.H. (1996) *Encyclopedia of climate and weather*, Oxford University Press New York.
- 712 Shi, K., Zhang, Y., Li, Y., Li, L., Lv, H. and Liu, X. (2015a) Remote estimation of
713 cyanobacteria-dominance in inland waters. *Water Research* 68(0), 217-226.
- 714 Shi, K., ZHANG, Y., Xu, H., Zhu, G., Qin, B., Huang, C., Liu, X., Zhou, Y. and Heng, L. (2015b)
715 Long-term satellite observations of microcystin concentrations in Lake Taihu during cyanobacterial
716 bloom periods. *Environmental science & technology*
717 49(11), 6448-6456.
- 718 Simis, S.G.H., Peters, S.W.M. and Gons, H.J. (2005) Remote sensing of the cyanobacterial pigment
719 phycocyanin in turbid inland water. *Limnology and Oceanography* 50(1), 237-245.
- 720 Simis, S.G.H., Ruiz-Verdu, A., Dominguez-Gomez, J.A., Pena-Martinez, R., Peters, S.W.M. and Gons,

- 721 H.J. (2007) Influence of phytoplankton pigment composition on remote sensing of cyanobacterial
 722 biomass. *Remote Sensing of Environment* 106(4), 414-427.
- 723 Smith, V.H. (1983) Low nitrogen to phosphorus ratios favor dominance by blue-green algae in lake
 724 phytoplankton. *Science* 221(4611), 669-671.
- 725 Sun, D.Y., Li, Y.M. and Wang, Q. (2009) A Unified Model for Remotely Estimating Chlorophyll a in
 726 Lake Taihu, China, Based on SVM and In Situ Hyperspectral Data. *Ieee Transactions on Geoscience*
 727 *and Remote Sensing* 47(8), 2957-2965.
- 728 Tao, M., Duan, H., Cao, Z., Loiselle, S. and Ma, R. (2017) A Hybrid Empirical Orthogonal Function
 729 Algorithm to Improve MODIS Cyanobacterial Phycocyanin Data Quality in a Highly Turbid Lake:
 730 Bloom and Non-bloom Condition. *Ieee Journal of Selected Topics in Applied Earth Observations and*
 731 *Remote Sensing*.
- 732 Tilman, D., Kiesling, R., Sterner, R., Kilham, S. and Johnson, F. (1986) Green, bluegreen and diatom
 733 algae: taxonomic differences in competitive ability for phosphorus, silicon and nitrogen. *Archiv Fur*
 734 *Hydrobiologie* 106(4), 473-485.
- 735 Tilman, D., Kilham, S.S. and Kilham, P. (1982) Phytoplankton Community Ecology: The Role of
 736 Limiting Nutrients. *Annual Review of Ecology and Systematics* 13, 349-372.
- 737 Tu, Q., Gu, D., Yin, C., Xu, Z. and Han, J. (1990) Chaohu Lake eutrophication study. Univ. Press of
 738 Sci. and Technol. of China, Hefei, China.
- 739 Tyler, A.N., Hunter, P.D., Carvalho, L., Codd, G.A., Elliott, A., Ferguson, C.A., Hanley, N.D.,
 740 Hopkins, D.W., Maberly, S.C., Mearns, K.J. and Scott, E.M. (2009) Strategies for monitoring and
 741 managing mass populations of toxic cyanobacteria in recreational waters: a multi-interdisciplinary
 742 approach. *Environmental Health* 8.

- UN (2006) Water: a shared responsibility. The United Nations World Water Development Report 2, UN-HABITAT.
- Wagner, C. and Adrian, R. (2009) Cyanobacteria dominance: Quantifying the effects of climate change. *Limnology and Oceanography* 54(6), 2460-2468.
- Wang, M., Nim, C.J., Son, S. and Shi, W. (2012) Characterization of turbidity in Florida's Lake Okeechobee and Caloosahatchee and St. Lucie Estuaries using MODIS-Aqua measurements. *Water Research* 46(16), 5410-5422.
- Wang, M. and Shi, W. (2007) The NIR-SWIR combined atmospheric correction approach for MODIS ocean color data processing. *Optics Express* 15(24), 15722-15733.
- Wang, M., Shi, W. and Tang, J. (2011) Water property monitoring and assessment for China's inland Lake Taihu from MODIS-Aqua measurements. *Remote Sensing of Environment* 115(3), 841-854.
- WHO, G. (2011) Guidelines for drinking-water quality. World Health Organization.
- Wynne, T.T., Stumpf, R.P. and Briggs, T.O. (2013) Comparing MODIS and MERIS spectral shapes for cyanobacterial bloom detection. *International Journal of Remote Sensing* 34(19), 6668-6678.
- Xu, F. (1997) Exergy and structural exergy as ecological indicators for the development state of the Lake Chaohu ecosystem. *Ecological Modelling* 99(1), 41-49.
- Xu, H., Paerl, H.W., Qin, B.Q., Zhu, G.W. and Gao, G. (2010) Nitrogen and phosphorus inputs control phytoplankton growth in eutrophic Lake Taihu, China. *Limnology and Oceanography* 55(1), 420-432.
- Xu, H., Qin, B., Zhu, G., Hall, N.S., Wu, Y. and Paerl, H. (2014) Determining critical nutrient thresholds needed to control harmful cyanobacterial blooms in hypertrophic Lake Taihu, China. *Environmental Science & Technology* 49, 1051-1059.

- 765 Xu, M., Cao, H., Xie, P., Deng, D., Feng, W. and Xu, J. (2005) The temporal and spatial distribution,
766 composition and abundance of Protozoa in Chaohu Lake, China: Relationship with eutrophication.
767 *European Journal of Protistology* 41(3), 183-192.
- 768 Yang, L., Lei, K., Meng, W., Fu, G. and Yan, W. (2013) Temporal and spatial changes in nutrients and
769 chlorophyll- α in a shallow lake, Lake Chaohu, China: An 11-year investigation. *Journal of*
770 *Environmental Sciences* 25(6), 1117-1123.
- 771 Yu, L., Kong, F., Zhang, M., Yang, Z., Shi, X. and Du, M. (2014) The Dynamics of Microcystis
772 Genotypes and Microcystin Production and Associations with Environmental Factors during Blooms
773 in Lake Chaohu, China. *Toxins* 6(12), 3238-3257.
- 774 Zhang, M., Zhang, Y., Yang, Z., Wei, L., Yang, W., Chen, C. and Kong, F. (2016) Spatial and seasonal
775 shifts in bloom-forming cyanobacteria in Lake Chaohu: Patterns and driving factors. *Phycological*
776 *Research* 64(1), 44-55.
- 777 Zhang, Y., Ma, R., Zhang, M., Duan, H., Loiselle, S. and Xu, J. (2015) Fourteen-Year Record (2000-
778 2013) of the Spatial and Temporal Dynamics of Floating Algae Blooms in Lake Chaohu, Observed
779 from Time Series of MODIS Images. *Remote Sensing* 7(8), 10523-10542.
- 780

Tabel 1. Water quality properties collected in Lake Chaohu. Chla: chlorophyll-a; PC: Cyanobacteria phycocyanin pigments; SPM: suspended particulate matter.

Date	N	Chla ($\mu\text{g/L}$)		PC($\mu\text{g/L}$)		SPM(mg/L)		PC:Chla	
		Mean	Range	Mean	Range	Mean	Range	Mean	Range
201305	56	42.50 \pm 55.58	8.19-257.65	130.79 \pm 190.87	12.48-909.92	38.21 \pm 17.27	10.00-92.86	4.62 \pm 7.48	0.55-50.39
201306	31	165.80 \pm 304.65	15.16-1229.83	513.56 \pm 1603.55	30.74-4807.72	79.06 \pm 63.24	27.00-324.00	2.46 \pm 0.79	1.45-4.36
201307	45	54.62 \pm 56.64	12.75-260.80	111.94 \pm 196.12	9.85-776.55	111.29 \pm 55.11	38.00-244.00	1.76 \pm 1.15	0.22-5.25
201309	25	160.83 \pm 251.75	20.11-1131.96	254.98 \pm 552.82	12.48-2682.32	50.12 \pm 26.33	20.00-138.00	1.17 \pm 0.56	0.46-2.66
201409	33	44.57 \pm 28.43	16.63-157.87	72.47 \pm 111.36	6.57-558.76	67.27 \pm 20.22	19.00-112.00	1.35 \pm 0.99	0.13-3.54
201501	30	54.36 \pm 36.89	17.86-138.55	42.50 \pm 55.97	9.85-321.27	31.80 \pm 10.05	12.00-65.00	1.10 \pm 0.98	0.09-4.11
201504	39	16.25 \pm 13.44	6.85-85.87	22.46 \pm 20.99	8.88-113.33	61.16 \pm 25.00	26.00-133.00	1.98 \pm 1.38	0.53-7.39

Table 2. Cyanobacterial risk levels in 5 km buffer zones around the drinking-water source in Lake Chaohu established from MODIS observations during 2000-2014 and a decision tree (Fig. S1). Note that blue means no risk, green means low risk, yellow means medium risk, and white means insufficient MODIS data available.

[illegible]

Fig.1 Location and distribution map of Lake Chaohu, China. Note that the red circle located near Chaohu City is 5 km surrounding zones around drinking-water source.

Fig.2 The processing procedure of MODIS Chla and PC products

Fig.3 Algorithm training and validations: (a) Chla training; (b) Chla validation; (c) PC training; (d) PC validation; (e) Chla error bar; (f) PC error bar.

Fig.4 Annual mean of (a) Chla, (b) PC and (c) PC:Chla ratio derived from MODIS for the three lake areas; (d) Annual mean of TN, TP and TN:TP for whole lake.

Fig.5 Monthly mean of (a) Chla, (b) PC and (c) PC:Chla ratio derived from MODIS for the three lake areas; (d) Monthly mean of TN, TP and TN:TP for whole lake.

Fig.6 Annual mean PC:Chla distributions derived from MODIS (2000-2014) in Lake Chaohu. Note that there are distinct boundary effects due to aerosol thicknesses (Tao et al., 2017), and long-term time-series data would contain some errors near the lake coast.

Fig.7 Monthly mean PC:Chla distributions derived from MODIS (2000-2014) in Lake Chaohu. Similar to annual mean PC:Chla product, there are distinct boundary effects due to aerosol thicknesses especially in summer seasons (Tao et al., 2017), and long-term time-series data would contain some errors near the lake coast.

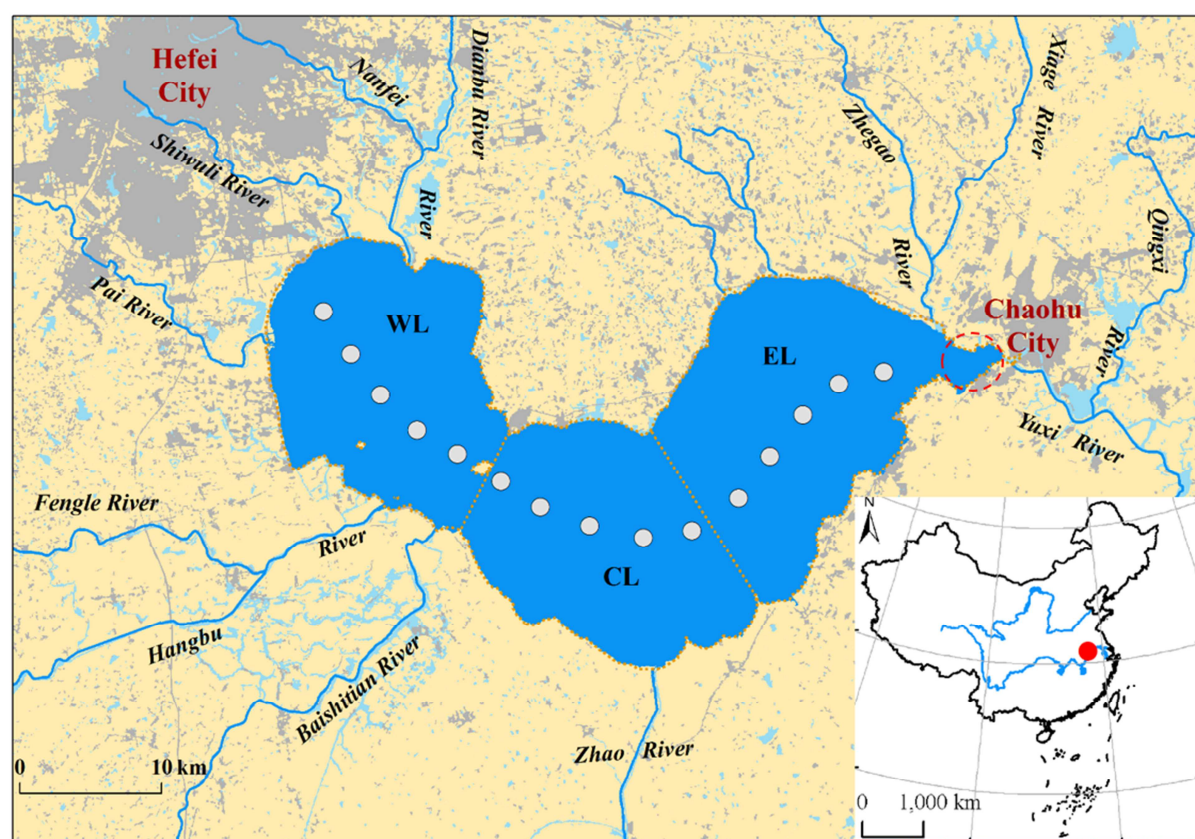
Fig.8 Time-series of satellite-derived phytoplankton pigments (a-c) and in situ measured nutrients (d-f) from the three lake segments. The long-time series nutrients data are provided by local Chaohu Management Bureau. Note that the blue dash line show the data with TN:TP larger than 29:1.

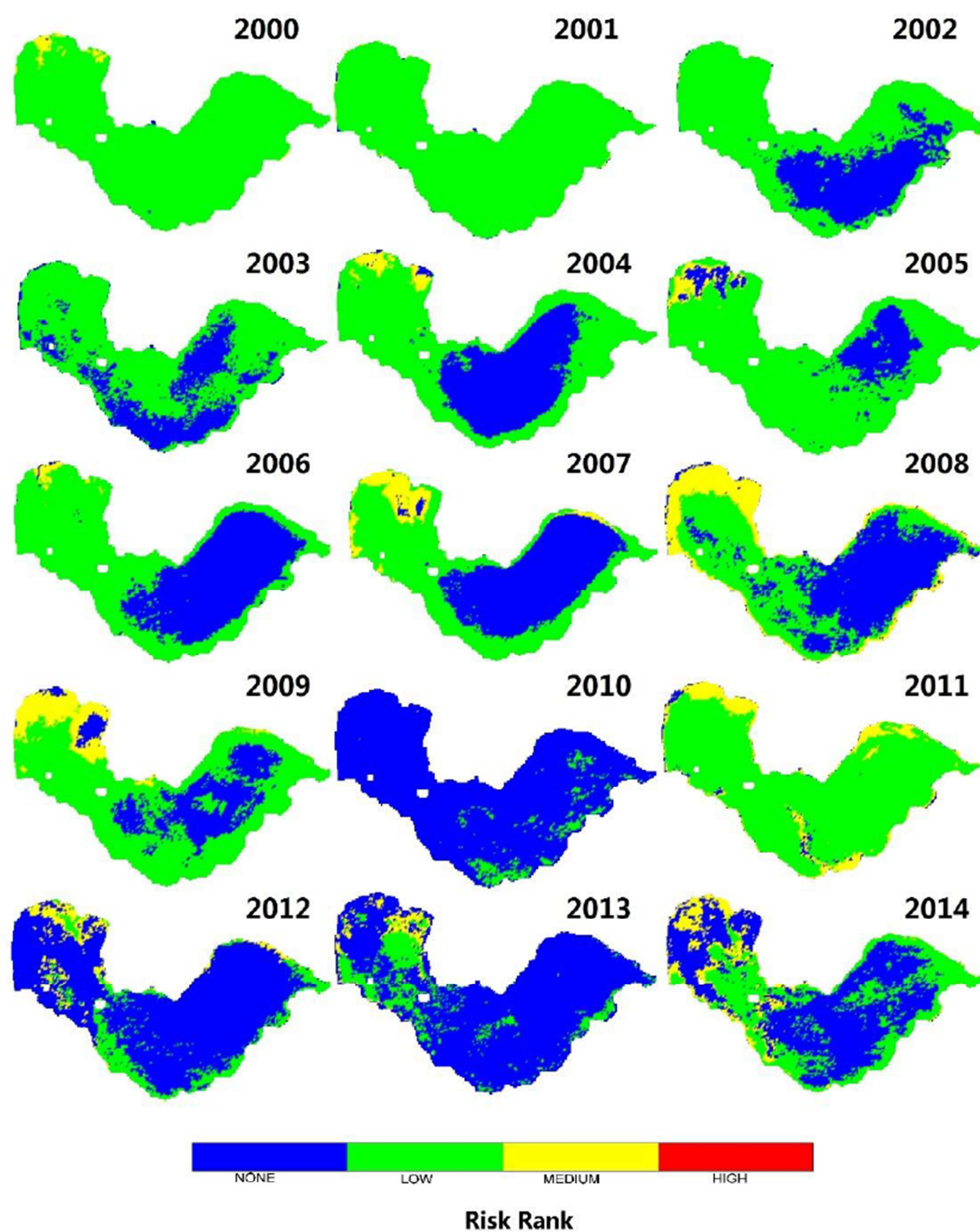
Fig.9 Relationship between (a) Chla, (b) PC and (c) PC:Chla and monthly mean temperature in entire lake.

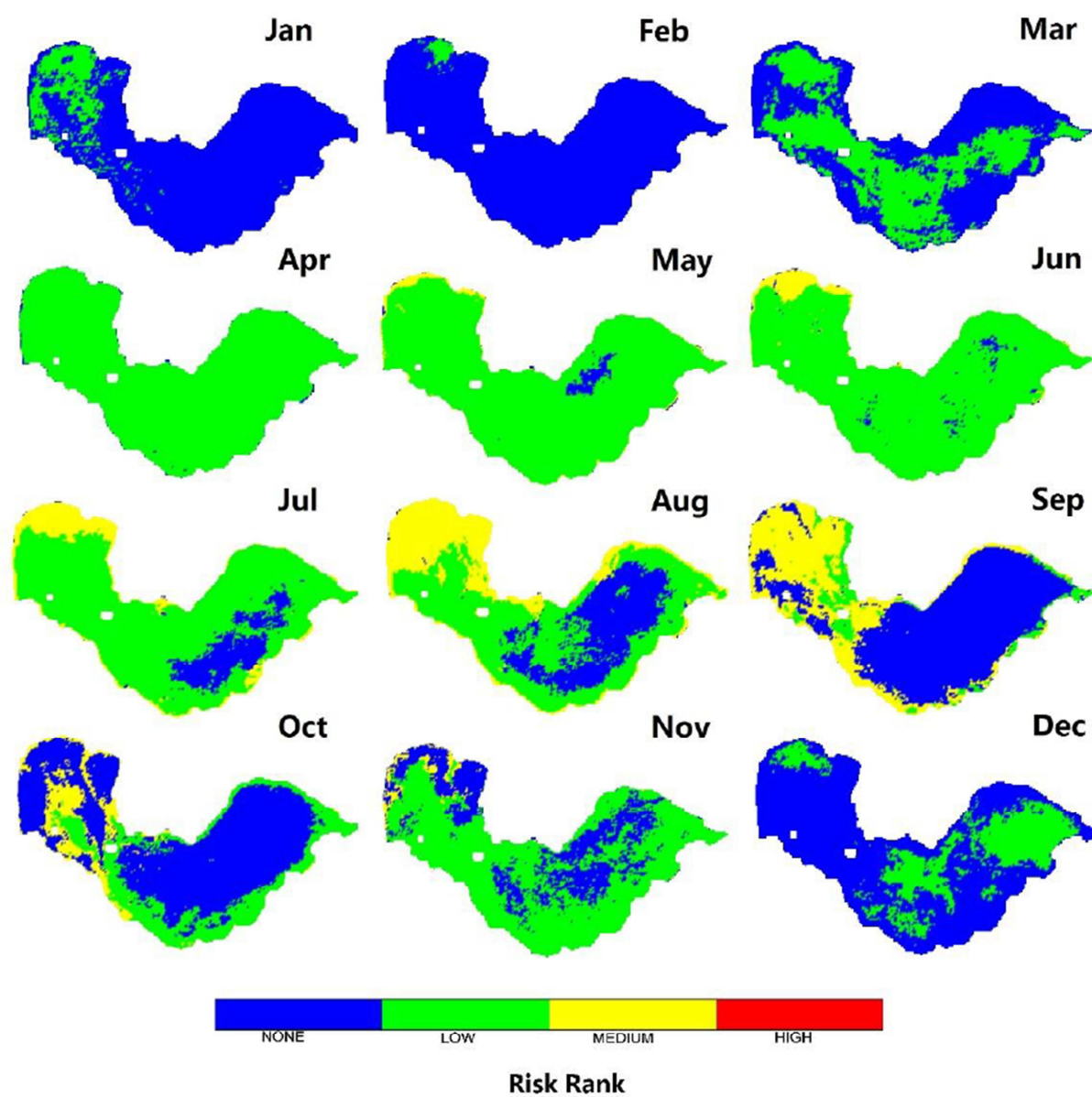
Fig.10 Annual mean risk rank distributions derived from MODIS (2000-2014) in Lake Chaohu.

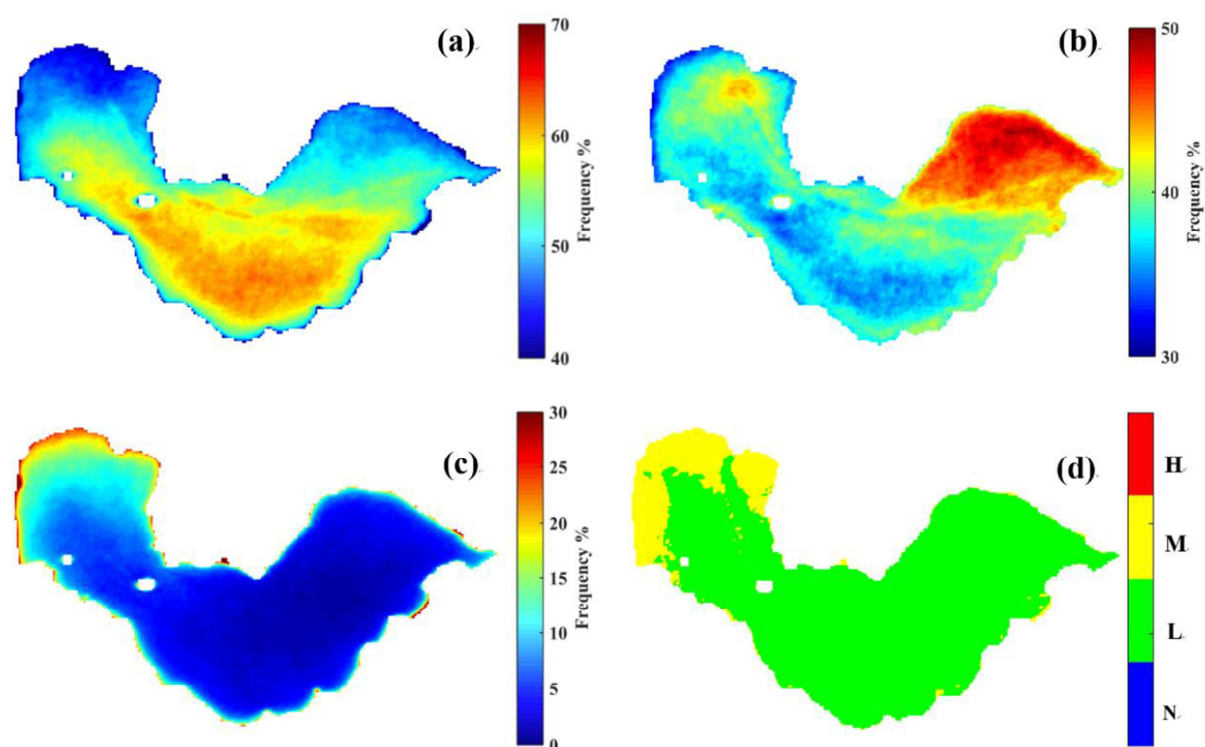
Fig.11 Monthly mean risk rank distributions derived from MODIS (2000-2014) in Lake Chaohu.

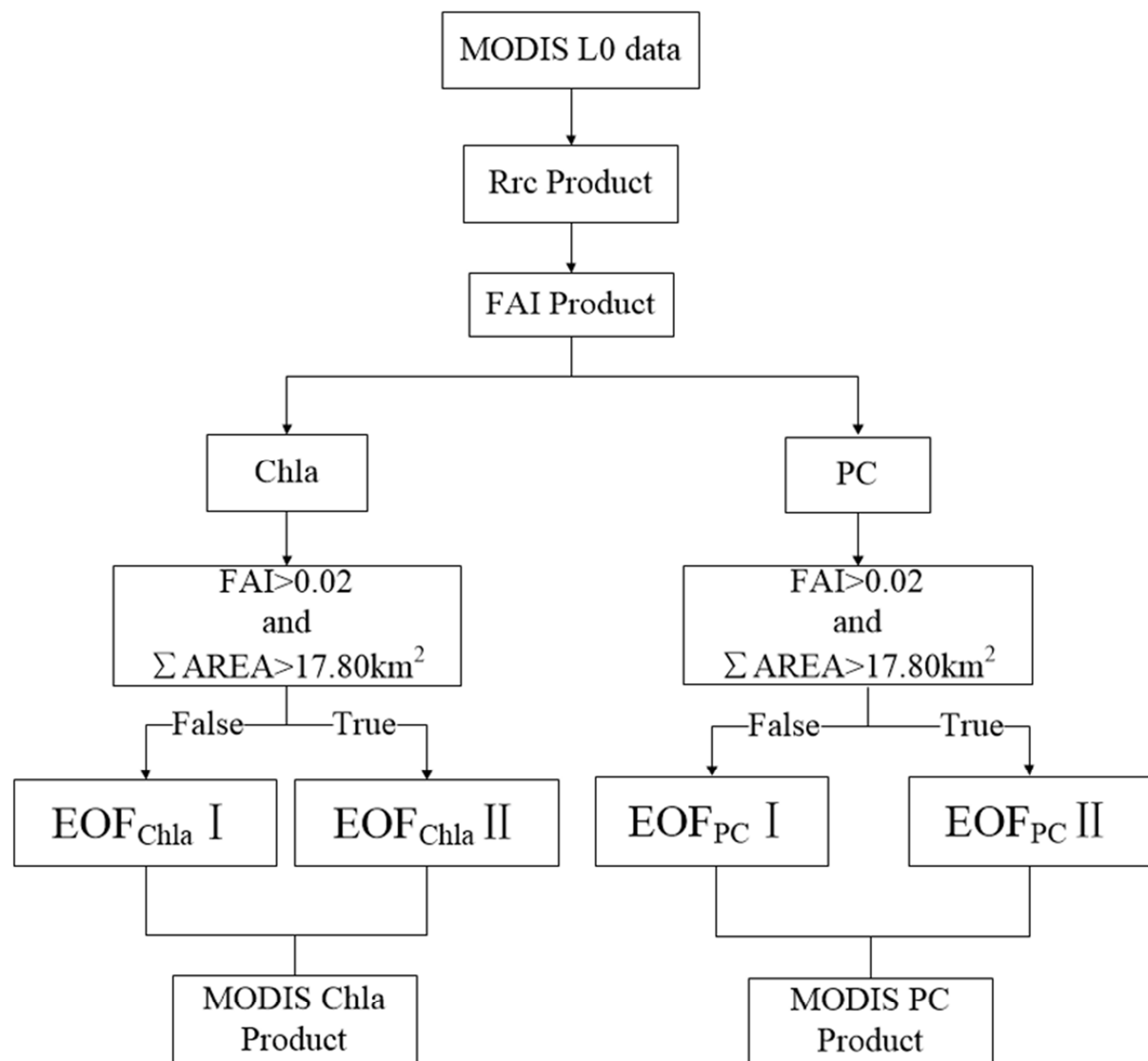
Fig.12 The frequency (a-c) and mean (d) of risk rank distributions derived from MODIS (2000-2014) in Lake Chaohu: (a) No (b) Low (c) Medium (d) Mean. Note that there is no high risk rank in Lake Chaohu.

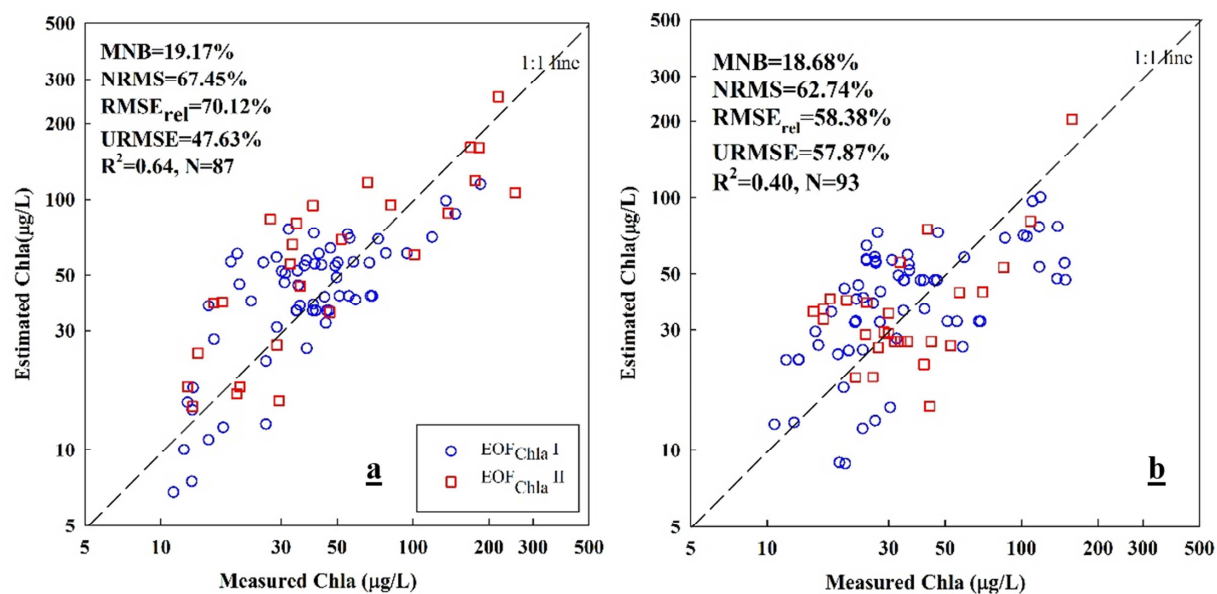


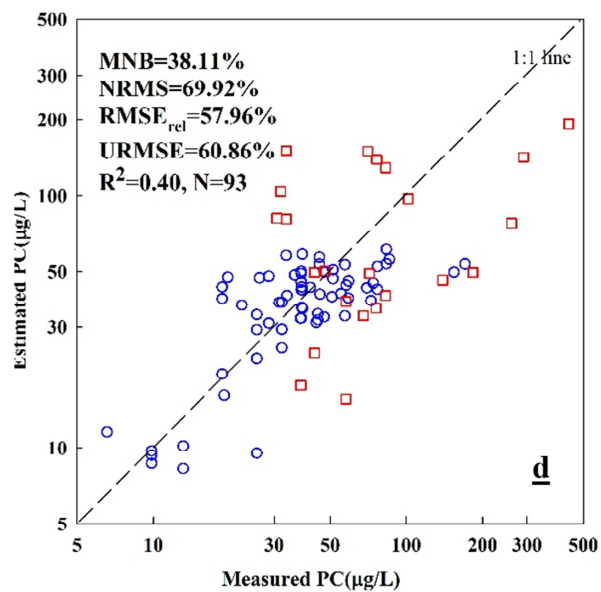
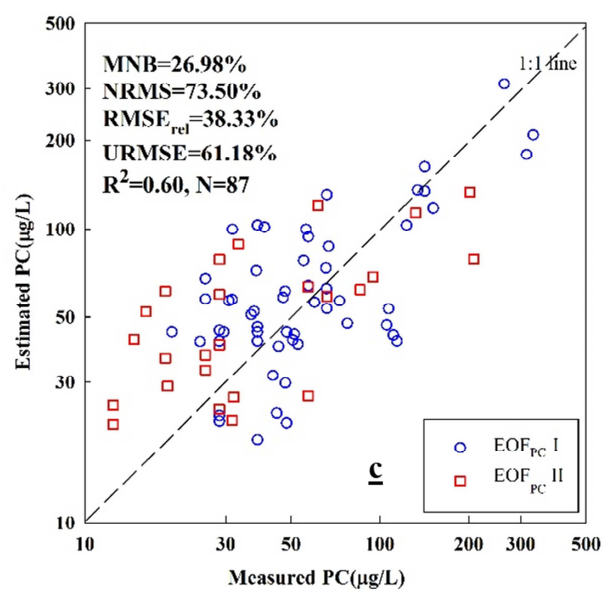


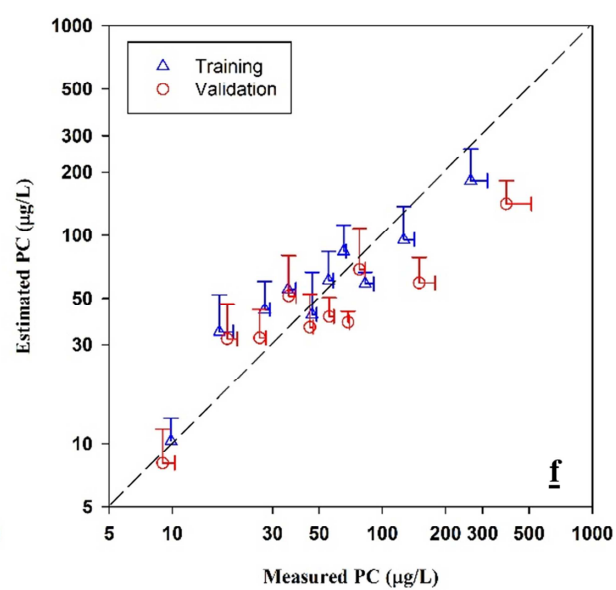
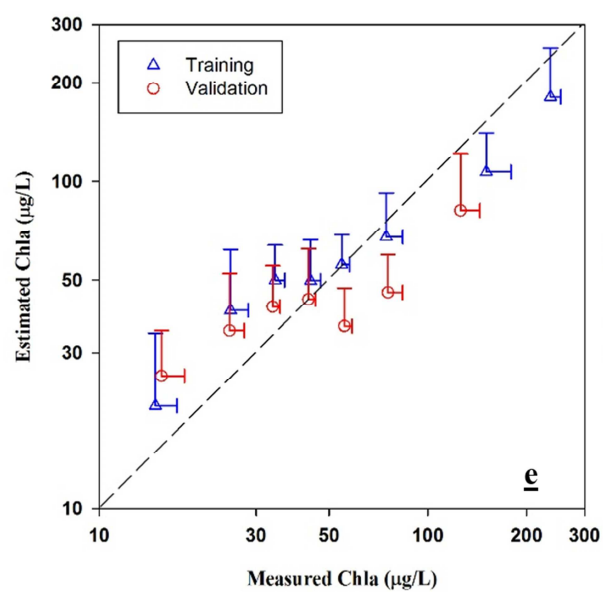


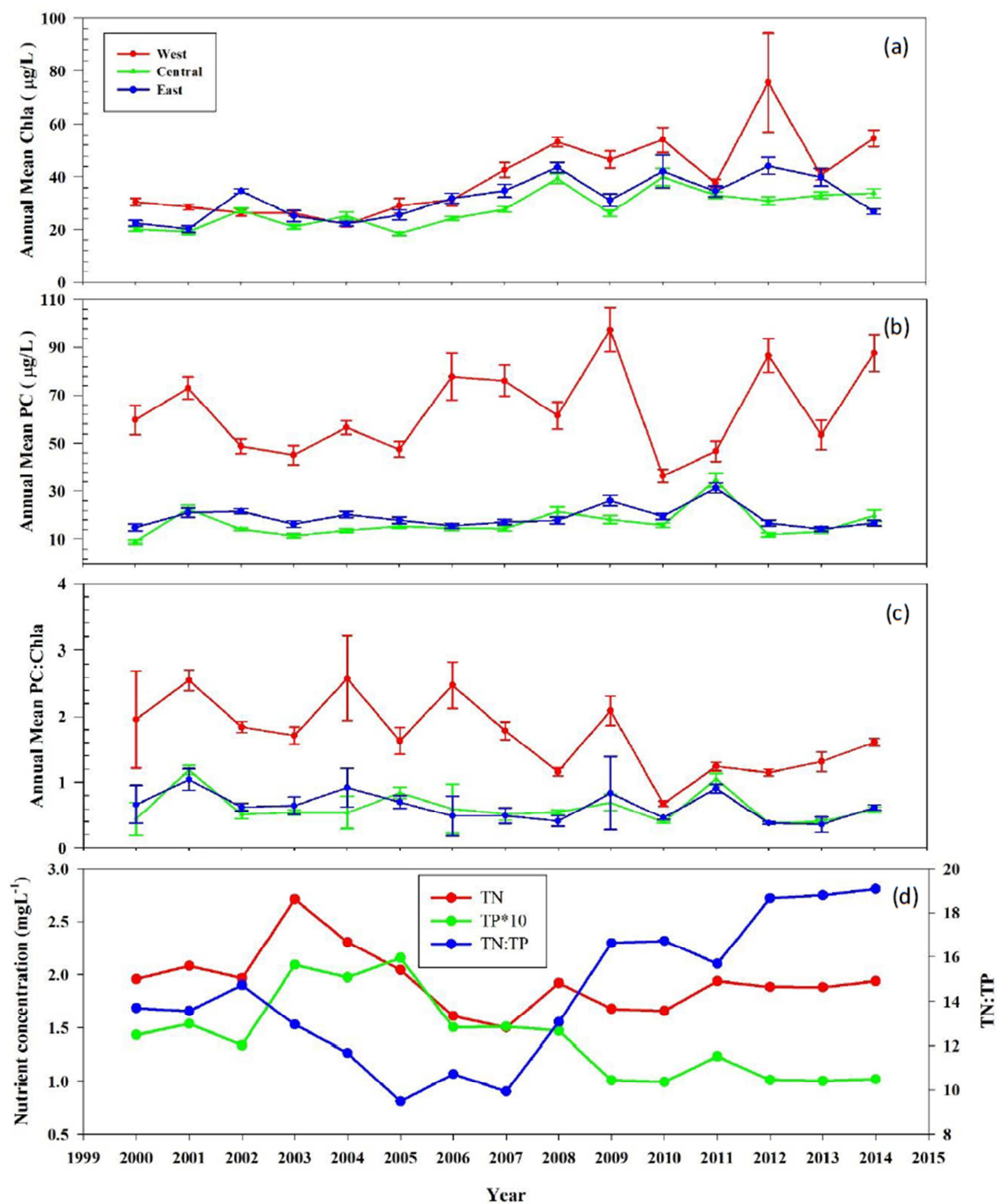


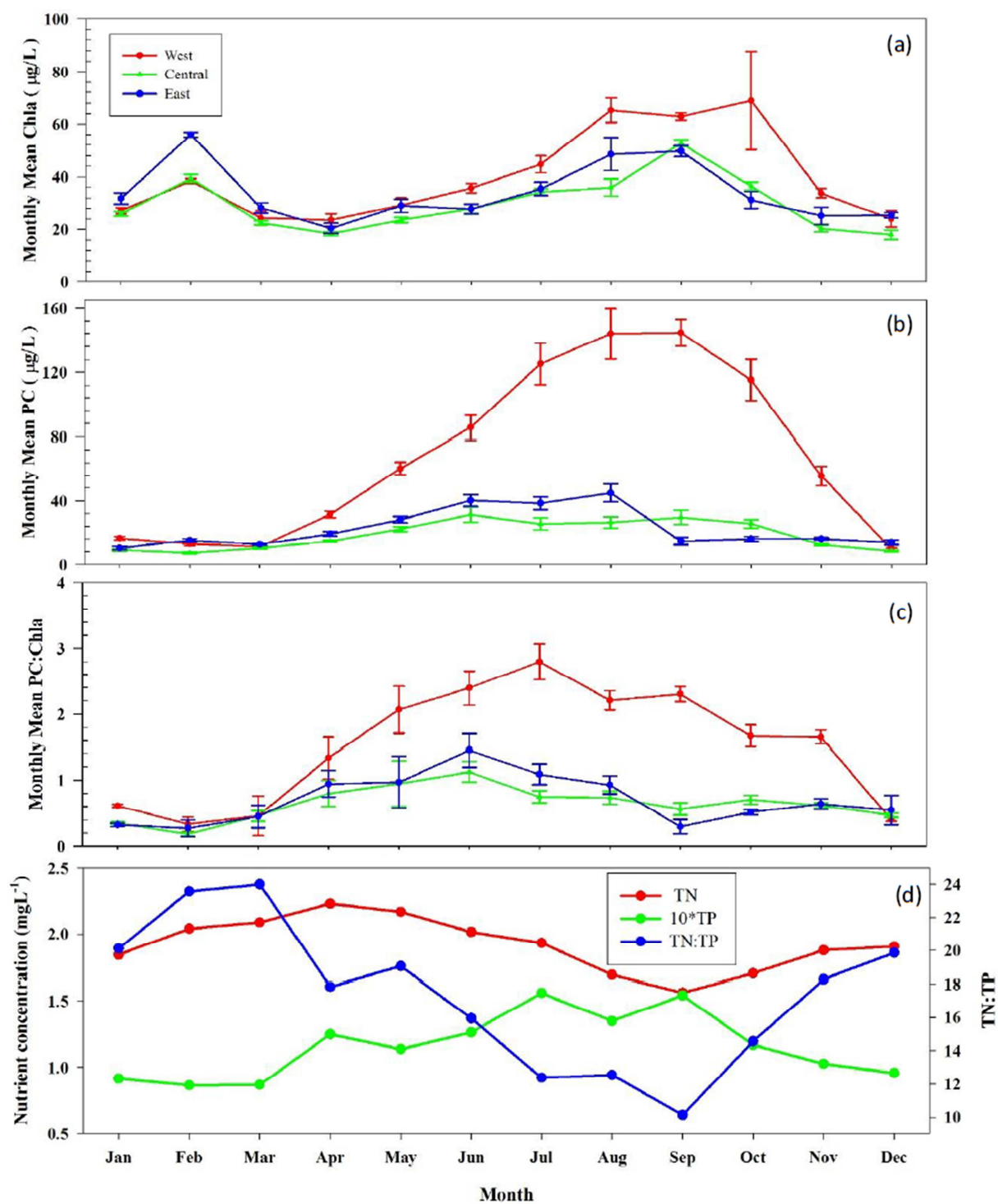


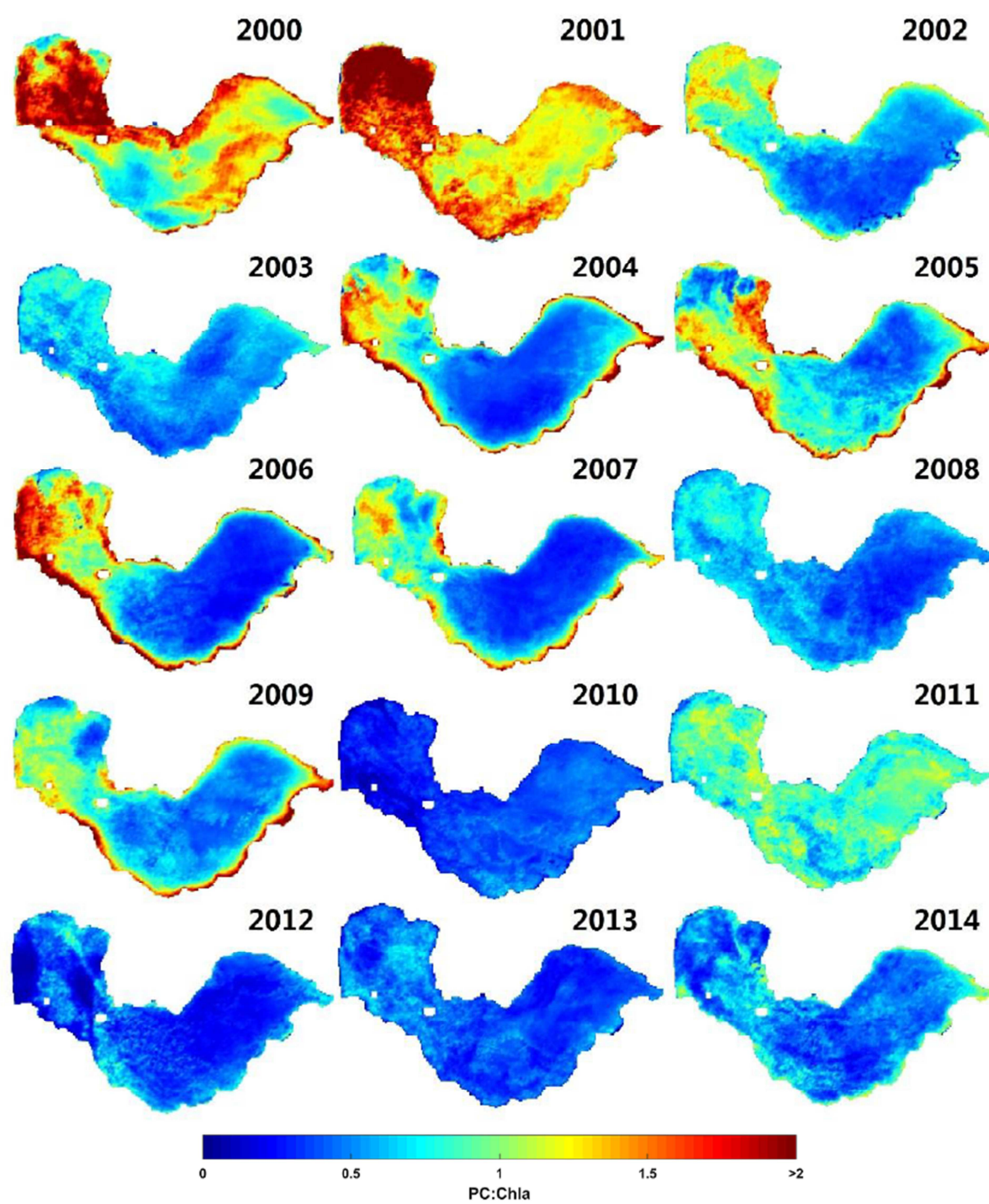


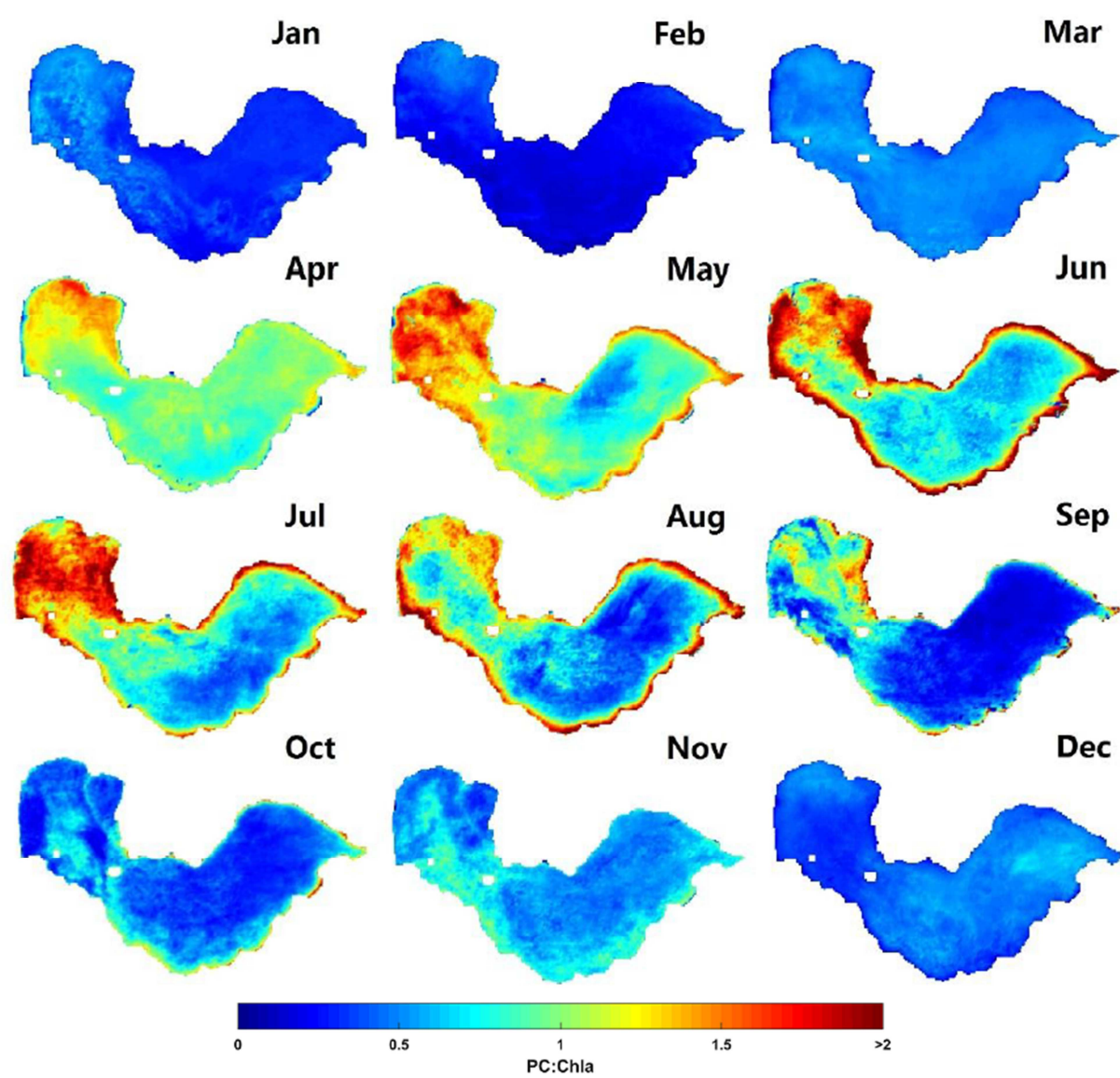


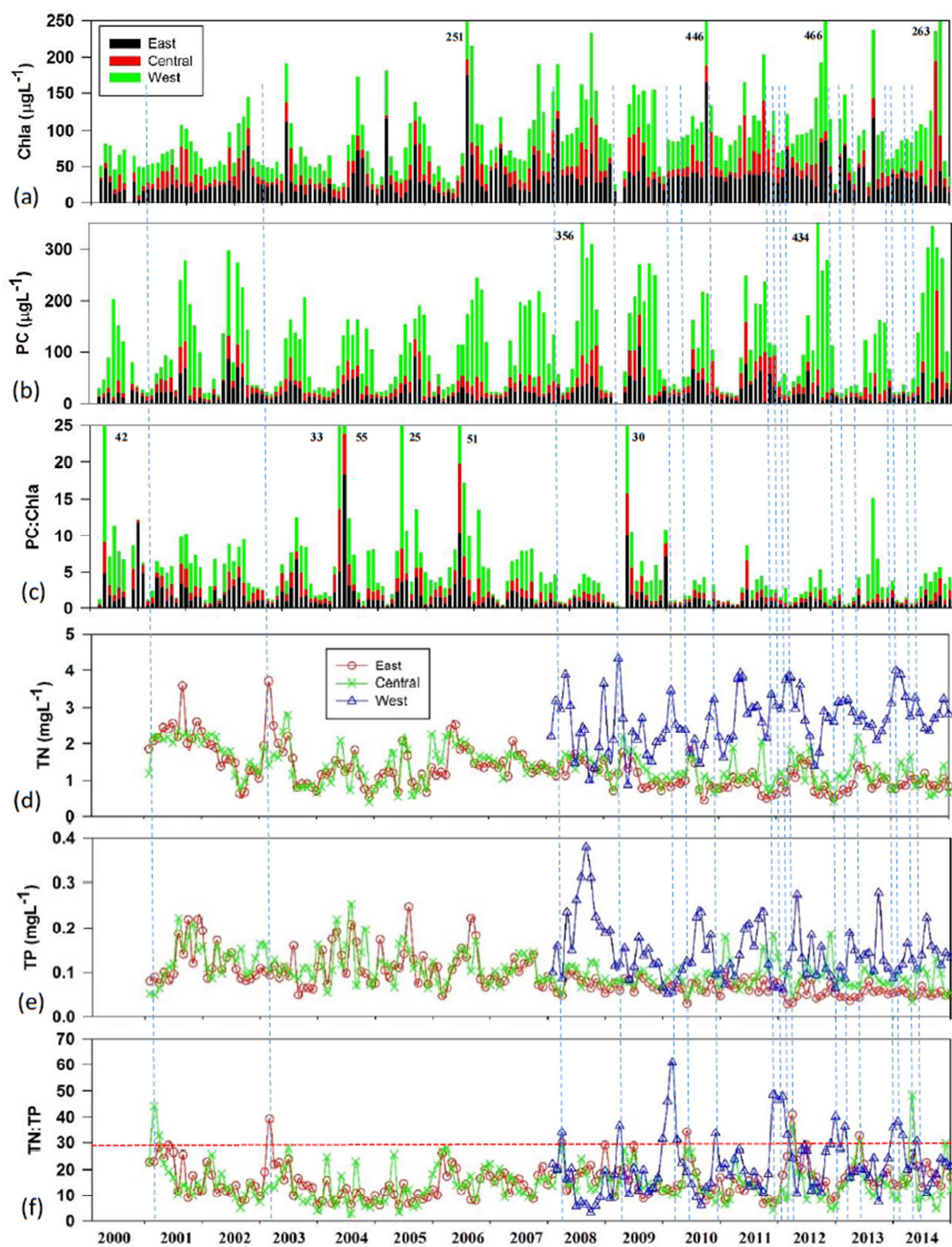


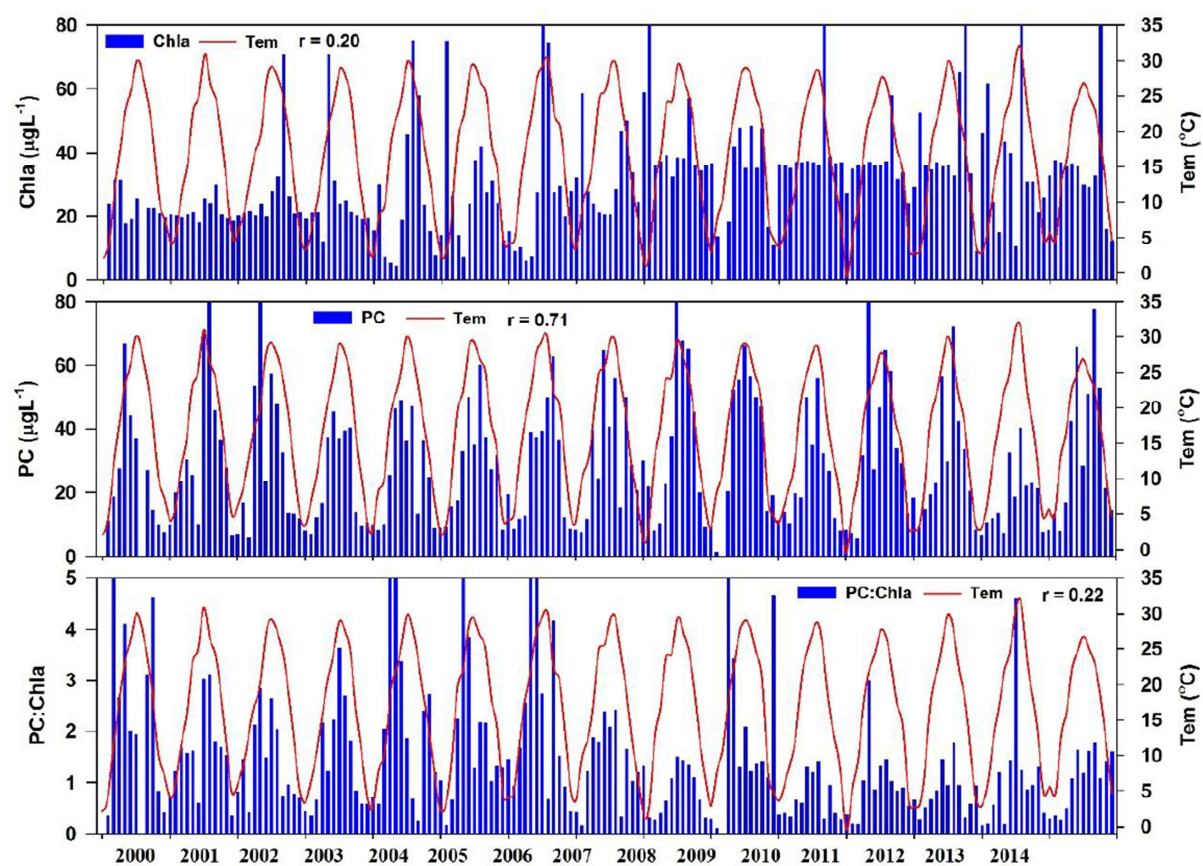












MODIS algorithms are developed to estimate chlorophyll a (Chla) and phycocyanin (PC) concentrations.

Long-term Chla, PC and PC:Chla maps are derived from 2000-2014 MODIS data in a eutrophic lake.

Low TN:TP and elevated temperatures influence the seasonal shift of phytoplankton community.

Cyanobacterial risk mapping provides a tool for safety evaluation in drinking-water source.